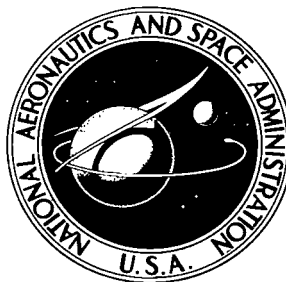


NASA TECHNICAL NOTE



NASA TN D-6041

2.1

NASA TN D-6041

LOAN COPY: RETU  
AFWL (WLOL)  
KIRTLAND AFB, TX

0132797



TECH LIBRARY KAFB, NM

TESTS OF A FULL-SCALE  
ANNULAR RAM-INDUCTION COMBUSTOR  
FOR A MACH 3 CRUISE TURBOJET ENGINE

*by Jerrold D. Wear, Porter J. Perkins,  
and Donald F. Schultz*

*Lewis Research Center  
Cleveland, Ohio 44135*



0132797

1. Report No. NASA TN D-6041		2. Government Accession No.		3. Recipient's Catalog No.	
4. Title and Subtitle TESTS OF A FULL-SCALE ANNULAR RAM- INDUCTION COMBUSTOR FOR A MACH 3 CRUISE TURBOJET ENGINE		5. Report Date October 1970		6. Performing Organization Code	
		8. Performing Organization Report No. E-5260		10. Work Unit No. 720-03	
7. Author(s) Jerrold D. Wear, Porter J. Perkins, and Donald F. Schultz		11. Contract or Grant No.		13. Type of Report and Period Covered Technical Note	
		14. Sponsoring Agency Code			
9. Performing Organization Name and Address Lewis Research Center National Aeronautics and Space Administration Cleveland, Ohio 44135		15. Supplementary Notes			
12. Sponsoring Agency Name and Address National Aeronautics and Space Administration Washington, D.C. 20546					
16. Abstract A 40-inch (1.02-m) diameter primary combustor 30 inches (0.76 m) long operated for 325 hours at simulated supersonic flight conditions with no loss in performance. Tests in a component facility were at inlet-air conditions of (1) 1150° F (894 K) and 90 psia (62.0 N/cm <sup>2</sup> ) (Mach 3.0) and (2) 1050° F (839 K) and 60 psia (41.4 N/cm <sup>2</sup> ) (Mach 2.7), with 2200° F (1478 K) exit temperatures. Some metal burning occurred. At Mach 3.0 conditions, combustion efficiency was 100 percent, pressure loss 7.4 percent, and exit temperature profiles good. Exit temperature pattern factors were 0.19 and 0.29 at Mach 3 and at simulated takeoff, respectively. These performance parameters (as well as altitude relight limits, heat flux, headplate temperatures, response to rapid increase in fuel flow, and exhaust smoke) were measured over a wide range of operating conditions.					
17. Key Words (Suggested by Author(s)) Hydrocarbon combustion    Combustors Combustion efficiency    Jet engine Ignition limits    Combustion			18. Distribution Statement Unclassified - unlimited		
19. Security Classif. (of this report) Unclassified	20. Security Classif. (of this page) Unclassified	21. No. of Pages 46	22. Price* \$3.00		

# TESTS OF A FULL-SCALE ANNULAR RAM-INDUCTION COMBUSTOR FOR A MACH 3 CRUISE TURBOJET ENGINE

by Jerrold D. Wear, Porter J. Perkins, and Donald F. Schultz

Lewis Research Center

## SUMMARY

A 40-inch (1.02-m) diameter primary combustor 30 inches (0.76 m) long was tested in a component test facility to evaluate endurance problems and to determine combustor performance. The combustor was designed for 1150° F (894 K) and 90 psia (62.0 N/cm<sup>2</sup>) inlet-air conditions (Mach 3.0 cruise) and for 2200° F (1478 K) exit temperatures. Testing was conducted at the design conditions and at 1050° F (839 K) and 60 psia (41.4 N/cm<sup>2</sup>) (Mach 2.7 cruise). The combustor was a modified version of that used in the Pratt & Whitney JTF-17 experimental supersonic transport engine. Scoops with turning vanes in the combustor liners induced ram air at relatively high velocity into the combustion and dilution zones.

A total of 325 hours of cyclic endurance testing was performed at the Mach 2.7 and 3.0 cruise conditions without loss of combustor performance. Some burned scoops, burned areas on the inner liner surfaces, and thermal stress cracks existed at the end of the 325 hours.

Combustion efficiency at design conditions was 100 percent and started dropping only at pressures below 30 psia (20.7 N/cm<sup>2</sup>), falling to 85 percent at 5 psia (3.4 N/cm<sup>2</sup>). Efficiency dropped at low inlet-air temperature, reaching 60 percent at 100° F (311 K).

Combustor pressure loss was 7.4 percent at design conditions for Mach 3 cruise and was affected by diffuser inlet velocity profile. A nonuniform inlet velocity profile (distorted toward the outer diameter) caused a higher pressure loss than that obtained with a uniform inlet velocity profile.

The exit radial temperature profile was in good agreement with the design profile and insensitive to diffuser inlet velocity profile changes. Exit temperature pattern factor was 0.29 and 0.19 for the simulated takeoff and Mach 3 cruise conditions, respectively.

Combustor relight limits at low pressures and temperature were determined. Also measured were heat flux and headplate temperatures. Exit temperature response to a rapid step increase in fuel flow was good. Smoke measurements indicate no visible smoke at cruise conditions and only slightly visible smoke at simulated takeoff.

## INTRODUCTION

Currently, there is great interest in commercial flight at Mach numbers of 3 and above. The conditions to which a turbojet engine is subject at such Mach numbers are severe. The combustor inlet-air temperature may exceed  $1100^{\circ}\text{ F}$  ( $867\text{ K}$ ) for an extended period of time. Such a high inlet-air temperature makes adequate cooling of the combustor liner difficult. The desired turbine inlet temperatures of  $2200^{\circ}\text{ F}$  ( $1478\text{ K}$ ) and above further jeopardize the life of the combustor.

A test program was conducted at the Lewis Research Center to evaluate the magnitude of the combustor endurance problem under severe conditions. A full-scale primary combustor designed for operation at Mach 3 cruise conditions was tested cyclically for more than 300 hours. In addition, the performance of the combustor was determined for a wide range of operating conditions.

## SCOPE OF INVESTIGATION

The purpose of this investigation was to determine the durability and performance characteristics of an annular combustor designed for operation at Mach 3 cruise conditions. The combustor tested was a modified version of one used by the Pratt & Whitney Aircraft Division, United Aircraft Corporation, in their experimental supersonic transport candidate engine, the JTF-17.

Tests were conducted with the full-scale full-annular combustor using ASTM-A-1 fuel at ambient temperatures in a connected-duct component test facility at the Lewis Research Center. Inlet-air temperatures up to  $1150^{\circ}\text{ F}$  ( $894\text{ K}$ ) were obtained without vitiation of the combustor air supply. The details of the test facility and the instrumentation are contained in appendixes A and B, respectively.

The results of the test program are presented in three parts as follows:

- (1) Combustor development: This section discusses the combustor modifications made to improve the performance to the desired level prior to the start of the endurance program.
- (2) Endurance tests: This section summarizes the major results obtained from 325 hours of cyclic endurance testing at average exit temperatures to  $2200^{\circ}\text{ F}$  ( $1478\text{ K}$ ).
- (3) Performance test: Combustion efficiency, pressure loss, and exit temperature profile data are presented for a range of inlet-air pressures and temperatures, reference velocities, and combustor fuel-air ratios. Data are also presented on combustor blowout and altitude relight limits, flame radiation, headplate temperatures, smoke characteristics, combustor response to a sudden increase in fuel flow, and the effect of inlet velocity profile on combustor airflow split and on exit temperature profile.

## COMBUSTOR DESCRIPTION

The combustor tested was designed using the ram-induction approach described in reference 1. A ram-induction combustor differs from conventional combustors in that the compressor discharge air is diffused less and the relatively high velocity air is captured by scoops in the combustor liner wall and turned into the combustion and mixing zones. Vanes are used in the scoops to reduce pressure loss caused by the high-velocity turns. The high velocity and steep angle of the entering air jets promote rapid mixing of the fuel and air in the combustion zone and of the burned gases and air in the dilution zone. The potential result of the rapid mixing is a shorter combustor or, alternatively, a better exit temperature profile in a given length.

The combustor with which the present investigation began is shown in cross section in figure 1. The outer housing diameter is approximately 42 inches (1.07 m), and the length from the compressor exit plane to the turbine inlet plane is approximately 30 inches (0.76 m). A forward snout on the combustor divides the diffuser into three concentric annular passages. The central passage conducts air to the combustor headplate, and the inner and outer passages supply air to the combustor inner and outer liners. There are five circumferential rows of scoops on each liner to turn the air into the combustion and dilution zones.

The snout and the combustor are shown in figure 2. Figure 2(a) is a view of the snout and the upstream end of the combustor. The V-shaped cutouts in the snout fit around struts in the diffuser. The circular holes through the snout wall are for the fuel nozzle struts. Figure 2(b) is a view looking upstream into the combustor. The scoops in the inner and outer liners can be seen as well as the openings in the headplate for the fuel nozzles and swirlers. Figure 2(c) gives a closer view of the inner and outer liners and headplate showing fuel nozzles and swirlers in place. Simplex nozzles were used for all tests. Figure 3 is a key to the circumferential locations of various components in the combustor.

Further details of the combustor and diffuser design are given in reference 2. The major combustor design dimensions and specifications are summarized in table I.

## CALCULATIONS

### Combustion Efficiency

Efficiency was determined by dividing the measured temperature rise across the combustor by the theoretical temperature rise. The exit temperatures were measured with 5-point traversing aspirated thermocouple probes and were mass-weighted for the efficiency calculation. The indicated readings of all thermocouples were taken as true

values of the total temperatures. The mass-weighting procedure is given in reference 2. In each mass-weighted average, 585 individual exit temperatures were used.

## Reference Velocity

Reference velocity for the combustor was computed from the total airflow, the maximum cross-sectional area between the inner and outer shrouds (see table I), and the air density based on the total pressure and temperature at the diffuser inlet.

## Total Pressure Loss

The total pressure loss was calculated by mass-averaging total pressures measured upstream of the diffuser inlet and at the combustor exit. The total pressure loss therefore includes the diffuser loss. The inlet Mach numbers used to correlate total pressure loss were determined from the inlet static pressures measured around the inlet annulus, the annulus area, and the measured airflow.

## Exit Temperature Profile Parameters

Three parameters of interest in evaluating the quality of exit temperature profile are considered. The first is the exit temperature pattern factor  $\bar{\delta}$  defined as

$$\bar{\delta} = \frac{T_{\text{exit,max}} - T_{\text{exit,av}}}{T_{\text{exit,av}} - T_{\text{inlet,av}}}$$

where  $T_{\text{exit,max}} - T_{\text{exit,av}}$  is the maximum temperature occurring anywhere in the combustor exit plane minus the average exit temperature. This is a useful parameter for preliminary screening but does not take into account the desired radial temperature profile for which the combustor was designed. Two other parameters do take the design profile into account. These parameters are

$$\delta_{\text{stator}} = \frac{(T_{R,\text{exit,local}} - T_{R,\text{exit,design}})_{\text{max}}}{T_{\text{exit,av}} - T_{\text{inlet,av}}}$$

$$\delta_{\text{rotor}} = \frac{(T_{R, \text{exit}, \text{av}} - T_{R, \text{exit}, \text{design}})_{\text{max}}}{T_{\text{exit}, \text{av}} - T_{\text{inlet}, \text{av}}}$$

where  $T_{R, \text{exit}, \text{local}} - T_{R, \text{exit}, \text{design}}_{\text{max}}$  for  $\delta_{\text{stator}}$  is the largest positive temperature difference between the highest local temperature at any given radius and the design temperature for that same radius; and where  $T_{R, \text{exit}, \text{av}} - T_{R, \text{exit}, \text{design}}_{\text{max}}$  for  $\delta_{\text{rotor}}$  is the largest temperature difference between the average radial temperature at any given radius and the design temperature for that same radius (ref. 3). The term  $T_{\text{exit}, \text{av}} - T_{\text{inlet}, \text{av}}$  used in all three parameters is the average temperature rise across the combustor.

The parameter  $\delta_{\text{stator}}$  is a measure of the effect of the quality of the exit temperature profile on the turbine stator, and  $\delta_{\text{rotor}}$  describes the effect of the quality of the exit temperature profile on the turbine rotor.

## RESULTS AND DISCUSSION

### Combustor Development

Development tests. - The combustor shown in figure 1, called the Model A combustor, was tested at a total pressure of 90 psia ( $62.1 \text{ N/cm}^2$ ), inlet-air temperatures to  $1150^\circ \text{ F}$  ( $894 \text{ K}$ ), and exit average temperatures to  $2200^\circ \text{ F}$  ( $1478 \text{ K}$ ). During limited operation at these conditions, the combustor showed areas of undesirably high surface temperatures as evidenced by metal discoloration and warpage. These areas were primarily on the headplate between fuel nozzles, on the side walls of the scoops on the inner liner, and on the outer liner just downstream of the third row of scoops.

Combustor modification. - The overheating of these areas was substantially reduced by the following minor modifications:

- (1) Addition of cooling slots in the headplate to cool the edges of the headplate (see fig. 2(c))
- (2) Addition of holes and an air deflector around each fuel nozzle to direct film cooling air over the surface of the headplate between the nozzles (see fig. 2(c))
- (3) More rigid support rings between the liners and the headplate to prevent liner warpage
- (4) Addition of cooling louvers (thumbnail scoops) to the combustor outer liner

In addition to the overheating problems encountered, the combustor showed hot spots in the exit temperature profile in line with the struts in the diffuser. It can be surmised that with a uniform fuel distribution these areas must have been deficient in airflow to

give a locally high fuel-air ratio and resulting high temperatures. The air deficiency could have come from the blockage effect or wake of the struts. The struts wakes tend to be accentuated by the action of the diffuser. Local regions of stalled flow might also have occurred in the diffuser, leading to further nonuniformity of airflow.

Correction of this problem required major changes to the diffuser and the combustor. A cross section of the combustor showing the changes is presented in figure 4. Walls were added in the diffuser to change the contour and reduce the rate of diffusion. In addition to the diffuser changes, the first row scoops were blocked entirely and one-third of each scoop in the fourth and fifth rows was also blocked. The increase in pressure loss resulting from the blocked scoops in the liner, along with the reduced diffusion in the diffuser, decreased the effect of the diffuser strut wakes on the temperature profile.

The changes in open area in all parts of the combustor and headplate that resulted from the modifications described are given in reference 2. The modified combustor in the final configuration is herein referred to as Model F to be consistent with the terminology of reference 2. The combustor open area was reduced from 352 square inches ( $2271 \text{ cm}^2$ ) to 289 square inches ( $1865 \text{ cm}^2$ ) by the modifications.

The isothermal total pressure loss of the Model A combustor was 3.6 percent at a diffuser inlet Mach number of 0.3. When the combustor open area was reduced to 289 square inches ( $1865 \text{ cm}^2$ ), the total pressure loss increased to 4.9 percent at the same diffuser inlet Mach number. The intermediate combustor modifications (Models B to E) leading to the final configuration are also described in reference 2.

The Model F combustor was considered to have adequate performance and sufficient durability potential to warrant more extensive endurance testing. Complete details of the development testing, summarized briefly in this section, can be found in reference 2.

## Endurance Tests

Description of endurance tests. - Cyclic endurance tests of the Model F combustor were conducted at the six test conditions given in table II. Cyclic operation was used to simulate the actual thermal cycling of the metal components.

The tests were conducted by operating the combustor in the following cyclic manner:

(1) Increase average exit temperature to the value called for in the test condition within 10 seconds after ignition.

(2) Maintain the test conditions for 1 hour.

(3) Reduce fuel flow to zero within 10 seconds.

(4) Wait a minimum of 5 minutes before starting the next operating cycle.



Tests were conducted for 1 hour at each of conditions 5 and 6 (table II) prior to the start of testing at condition 1, and again after completion of endurance testing at each of the conditions 1 to 4. This provided a check on the quality of the exit temperature profile at conditions of high temperature rise, where deterioration of the exit temperature profile would be more obvious.

A summary of the test time devoted to each operating condition is given in table II. A total of 325 hours of endurance testing was accumulated. The following is a brief summary of the effects of this extended severe testing on the combustor. Information in greater detail can be found in reference 2.

Results of endurance tests. - After 35 hours of cyclic operation at test condition 1, the combustor had no burned metal and no significant distortion. Following 100 hours of operation at test condition 2, the only deterioration noted was slight burning of a scoop in the third row on the inner liner and six small inner liner cracks. All cracks were from 1/4 to 3/4 inch (0.64 to 1.91 cm) long and originated at the thumbnail scoops. Holes 0.10 inch (0.25 cm) in diameter were drilled at the ends of the cracks to reduce concentrated stress and thereby stop further crack propagation. Testing was then conducted at test condition 3 for 30 hours. Following this test condition, examination showed that more cracks had developed in the outer liner, as well as in the inner liner. None of these cracks appeared to be serious from either a structural or performance standpoint. Testing was then conducted at test condition 4 for 45 hours prior to the next inspection. At that time there was additional burning of third row scoops on the inner liner. Also noted were additional cracks and lengthening of some of the previous cracks in the liners. The majority of the additional cracks were 3/8 inch (0.95 cm) or less in length. Testing was resumed at test condition 4, and the combustor was inspected again after a cumulative total of 98 hours at this condition. Several new cracks and further elongation of previous cracks were noted. Additional burning of third row scoops had also occurred. Testing was resumed at condition 4 until the cumulative total time at that condition was 150 hours.

Final examination of the combustor revealed some areas of extensive burning of the inner liner and the inner third row scoops. The most seriously burned area is shown in figures 5(a) and (b). Burning in these areas may have been caused by a lack of proper airflow to the inner liner of the combustor. Measurements confirmed that airflow to the inner liner was less than designed. These measurements are described in a later section of this report. Small cracks in the headplate were also found, extending from several of the cooling slots on the inner diameter. Some of the cooling air deflectors around the fuel nozzles were cracked and slightly burned. The exit transition cooling liners showed no evidence of deterioration.

The combustion efficiency, total pressure loss, exit temperature profile and pattern factor parameters as given in table II were not affected by the physical deterioration of the combustor. Thus, performance of a turbojet engine with this combustor would not

have changed during the 325-hour operation, even though physical deterioration had occurred.

## Performance Tests

Following the endurance testing, the Model F combustor was repaired. Burned scoops and liner areas were replaced to restore the combustor to its original condition. Tests were then conducted over a wider range of operating conditions to determine the combustor performance more completely. Experimental results obtained at the various operating conditions are listed in table III.

Combustion efficiency. - The effect of combustor pressure on combustion efficiency is shown in figure 6. The nominal operating conditions for these tests were an inlet-air temperature of  $600^{\circ}\text{F}$  ( $589\text{ K}$ ) and a reference velocity of 150 feet per second ( $45.7\text{ m/sec}$ ). Combustor pressure was varied from 60 to 5 psia ( $41.4$  to  $3.4\text{ N/cm}^2$ ). As shown in figure 6, the combustion efficiency was essentially 100 percent at all pressures above 30 psia ( $20.7\text{ N/cm}^2$ ) and decreased to approximately 85 percent as the combustor pressure was reduced to 5 psia ( $3.4\text{ N/cm}^2$ ). Three different sets of simplex-type fuel nozzles were used in these tests, designed to produce a 90 degree angle hollow cone spray. At the lower combustor pressures, the required fuel flow decreased so that smaller nozzles were needed to maintain an adequate pressure drop across the nozzles for good fuel atomization. A minimum fuel nozzle pressure differential of 40 psid ( $27.6\text{ N/cm}^2$ ) was arbitrarily used to ensure good atomization. The fuel flow pressure characteristics of these three fuel nozzles sets are shown in figure 7.

Further tests showed that, at pressures above 30 psia ( $20.7\text{ N/cm}^2$ ) and inlet-air temperatures above  $600^{\circ}\text{F}$  ( $589\text{ K}$ ), the combustion efficiency was 100 percent with variations in combustor reference velocity from 125 to 200 feet per second ( $38.1$  to  $61.0\text{ m/sec}$ ) and values of fuel-air ratio from 0.010 to 0.0254.

Inlet-air temperature had a marked effect on combustion efficiency, as shown in figure 8. At a pressure of 30 psia ( $20.7\text{ N/cm}^2$ ) and a reference velocity of 153 feet per second ( $46.6\text{ m/sec}$ ), the efficiency dropped from 100 to 60 percent as the inlet temperature decreased from  $600^{\circ}\text{F}$  to  $100^{\circ}\text{F}$  ( $589$  to  $311\text{ K}$ ).

Total pressure loss. - The combustor total pressure loss expressed as the percent of the average diffuser inlet total pressure is shown as a function of the diffuser inlet Mach number in figure 9. The two curves shown are data obtained without combustion (isothermally) and with a combustor temperature rise of approximately  $1150^{\circ}\text{F}$  ( $639\text{ K}$ ). The test conditions were a total pressure of 60 psia ( $41.4\text{ N/cm}^2$ ), inlet-air temperature of  $1050^{\circ}\text{F}$  ( $839\text{ K}$ ) and a range of reference velocities from 125 to 200 feet per second ( $38.1$  to  $61.0\text{ m/sec}$ ). The diffuser inlet velocity profile was uniform across the inlet annulus for these tests.

As previously stated, all the endurance testing was done with the diffuser inlet velocity pressure profile skewed toward the outer diameter. During this phase of the testing, the diffuser inlet velocity profile was varied. Three velocity pressure profiles used are shown in figure 10 and were a uniform profile, a profile skewed toward the outer diameter and a profile skewed toward the inner diameter. The skewed profiles were center or symmetrically peaked; however, the velocity pressure was higher near the wall that the profile was skewed or distorted toward. The distorted profiles were obtained by placing screens in the annulus ahead of the diffuser inlet. The effect of these air velocity profiles on the combustor total pressure loss is shown in figure 11. The total pressure loss is given at various airflow rates rather than the diffuser inlet Mach number as no single Mach number can fully represent the distorted velocity profiles. The effect of the distorted velocity profiles was to increase the combustor pressure loss at a given airflow rate. For example, at an airflow rate of approximately 77 pounds per second (35 kg/sec), the combustor isothermal total pressure loss was 5.6 percent with a uniform velocity profile, 6.8 percent with the profile skewed toward the outer diameter, and 7.8 percent with the profile skewed toward the inner diameter.

Effect of inlet-air velocity profile on combustor airflow distribution. - Isothermal tests were conducted to determine the effect of the three different inlet-air velocity profiles shown in figure 10 on the percent of total airflow in each of the three combustor flow passages. Inlet-air pressure and temperature for these tests were approximately 30 psia ( $20.7 \text{ N/cm}^2$ ) and  $300^\circ \text{ F}$  ( $422 \text{ K}$ ). The reference velocity was varied from about 50 to 170 feet per second (15.2 to 51.8 m/sec).

The airflow in the combustor inner, outer, and center flow passages was measured by total and static pressure instrumentation described in appendix B. The outer and inner flow passages each have about 38 percent of the total area, and the center passage, or snout, has the remaining 24 percent of the total area.

Results at inlet reference velocities of 90 to 100 feet per second (27.4 to 30.5 m/sec) are presented in table IV. With a uniform air velocity profile, the distribution of flow in the three passages agreed with the passage available flow area. The largest changes occurred when the air velocity profile was distorted to the outer diameter. Compared to the uniform air velocity profile, the inner passage flow decreased sharply and the center and outer passage flows increased considerably.

Discussion in the section on Results of endurance tests pointed out that there was extensive burning of the inner liner at the third row scoops and the possible reason for it. The endurance tests were conducted with the inlet-air-velocity pressure profile distorted to the outer diameter, which is characteristic of the compressor discharge of the JTF-17 engine. With this profile, the low airflow through the inner annulus as compared to the design flow may have resulted in insufficient cooling of the inner liner and scoops.

Exit temperature profile. - The desired average radial distribution of temperature at the combustor exit plane is determined by the stress and cooling characteristics of the

turbine. For purposes of evaluating the present combustor, exit radial temperature profiles were selected for both cruise and takeoff conditions that are typical of the JTF-17 design and other advanced engines. The measured average radial temperature profile is compared with the design radial profile in figure 12. Also shown is the maximum temperature measured at any point around the circumference for five radial positions. This provides an indication of the hot spots in the exit temperature profile.

Figure 12(a) presents results at an inlet-air temperature of  $1150^{\circ}\text{F}$  ( $894\text{ K}$ ), inlet-air pressure of  $90\text{ psia}$  ( $62.1\text{ N/cm}^2$ ), reference velocity of  $145\text{ feet per second}$  ( $44.2\text{ m/sec}$ ), and an exit average temperature of  $2200^{\circ}\text{F}$  ( $1478\text{ K}$ ) (Mach 3.0 cruise condition). The inlet velocity pressure profile was distorted toward the outer diameter. The agreement with the design profile is very good. The data of figure 12(b) are at an inlet-air temperature of  $600^{\circ}\text{F}$  ( $589\text{ K}$ ), inlet-air pressure of  $90\text{ psia}$  ( $62.1\text{ N/cm}^2$ ), reference velocity of  $100\text{ feet per second}$  ( $30.5\text{ m/sec}$ ), and an exit average temperature of  $2200^{\circ}\text{F}$  ( $1478\text{ K}$ ) (simulated takeoff condition). Since the average temperature was  $2200^{\circ}\text{F}$  ( $1478\text{ K}$ ) for both conditions, the combustor temperature rise was greater for the lower inlet-air temperature. This resulted in a greater deviation from the design profile as shown in figure 12(b). However, the measured average temperature profile did not differ from the design profile by more than  $60^{\circ}\text{F}$  ( $33\text{ K}$ ) in either case, except near the hub for the  $600^{\circ}\text{F}$  ( $589\text{ K}$ ) inlet-air temperature condition.

The deviation between the maximum measured temperature around the circumference and the design profile was significantly greater for the higher temperature rise. For the low-temperature-rise condition (high inlet-air temperature), the maximum temperature did not exceed the design profile by more than  $150^{\circ}\text{F}$  ( $83\text{ K}$ ). For the high-temperature-rise condition (low inlet-air temperature), the maximum temperature exceeded the design profile by about  $420^{\circ}\text{F}$  ( $233\text{ K}$ ).

The circumferential variation of exit temperature is shown in figure 13 for the two operating conditions of figure 12. The temperatures are averages of five radially spaced temperature measurements taken every  $3^{\circ}$  around the circumference. No correlation is apparent in figure 13 in the alinement of the local temperature peaks and the diffuser struts or fuel nozzles.

The exit radial temperature profiles were not significantly affected by moderate changes in diffuser inlet velocity profiles or by changes in reference velocity. This is evident in the similarity of the temperature profiles obtained with inlet velocity profiles undistorted and those distorted to the annulus outer and inner diameters, as shown in figure 14. For each inlet velocity profile, temperature profiles were obtained at four reference velocities:  $125$ ,  $150$ ,  $175$ , and  $200\text{ feet per second}$  ( $38.1$ ,  $45.7$ ,  $53.3$ , and  $61.0\text{ m/sec}$ ). The temperature profiles were measured at the Mach 2.7 cruise condition with a  $2200^{\circ}\text{F}$  ( $1478\text{ K}$ ) average outlet temperature. The greatest variation in the exit temperature profiles was caused by shifting the air velocity profile distortion from

the inner to the outer diameter. This caused a variation of  $75^{\circ}\text{ F}$  ( $41.7\text{ K}$ ) at the hub position. Near the center of the exit annulus, the temperature deviations differed by only about  $25^{\circ}\text{ F}$  ( $13.9\text{ K}$ ) for all velocity profiles.

Data presented in table IV show a considerable difference in airflow in the three inlet flow passages with change in inlet velocity profiles. However, the combustor exit temperature profile is shown in figure 14 to be generally insensitive to these airflow differences. For a decrease of inner annulus airflow from 38 to 22 percent of total flow when the velocity profiles were changed from uniform to one distorted to the outer diameter, the exit temperature near the hub increased only about  $60^{\circ}\text{ F}$  ( $33\text{ K}$ ).

The airflow profiles that are shown in figure 10, though distorted, are still essentially symmetric. To further evaluate combustor performance with distorted inlet velocity profiles, the velocity profile shown in figure 15 was used. This profile, similar to those used in reference 4, was unsymmetrically distorted toward the outer diameter. The combustor exit temperature profile obtained with this inlet velocity profile is compared to the desired profile in figure 16. The distorted inlet velocity profile did not cause much shift in the exit temperature profile. As expected, the tip was cooler than desired, but only by  $50^{\circ}\text{ F}$  ( $27.8\text{ K}$ ). The profile toward the hub was also cooler than desired, but only by  $30^{\circ}\text{ F}$  ( $16.7\text{ K}$ ). Maximum temperatures around the circumference were comparable to those shown in figure 12. This indicates that the combustor exit temperature profile is very insensitive to inlet airflow velocity profiles.

Combustor blowout and altitude relight. - To obtain blowout data, the combustor was first ignited at moderate inlet-air pressure. Then the pressure was lowered in steps while the inlet-air temperature, fuel-air ratio, and reference Mach number were held constant. After each change in pressure, a fuel burst test (rapid increase in fuel-air ratio) was made to determine whether the combustor would produce a corresponding temperature rise. This procedure indicates whether an engine would accelerate at these conditions. The fuel-air ratio would then be returned to the original value, the pressure reduced a further step, and the procedure repeated. Finally, at some pressure level, the combustor would be expected to blow out. However, the facility limited testing to a minimum pressure of  $4.5\text{ psia}$  ( $3.1\text{ N/cm}^2$ ), which at most inlet air temperatures was not low enough for blow out to occur. In these cases the combustor fuel was shut off. Relight was then attempted at successively increased pressure levels. If relight occurred, a fuel burst test was conducted at that condition to determine again if engine acceleration would occur.

The facility limited testing to a minimum inlet-air temperature of  $65^{\circ}\text{ F}$  ( $292\text{ K}$ ). All tests were conducted at a reference Mach number of 0.1 and a fuel-air ratio of 0.01. This corresponded to a temperature rise of about  $700^{\circ}\text{ F}$  ( $389\text{ K}$ ). The fuel burst tests increased the fuel-air ratio sufficiently to give a theoretical temperature rise of  $1000^{\circ}\text{ F}$  ( $555\text{ K}$ ).

Figure 17 presents the results of these tests. The limit line shown is for successful combustor relight followed by successful temperature rise. At inlet-air temperatures as low as 300° F (422 K), relight was possible down to a pressure of 5.0 psia (3.45 N/cm<sup>2</sup>) (approx. test facility limit). Below 300° F (422 K), increased combustor pressure was required for relight. At 90° F (300 K), the minimum pressure for relight was 8 psia (5.5 N/cm<sup>2</sup>) and increased sharply as the temperature was lowered to 65° F (292 K). No attempt was made to improve the relight characteristics of this combustor. Combustion was maintained at many conditions more severe than those at which relight was possible. Only one blowout point was reached within the limits of the facility. This occurred during a fuel burst at an air temperature of 75° F (297 K) and a pressure of 5 psia (3.4 N/cm<sup>2</sup>). One point of audible combustion instability occurred during a fuel burst test at 8 psia (5.5 N/cm<sup>2</sup>), 115° F (319 K) inlet-air temperature, and a fuel-air ratio of 0.018. In engine operation the combustor would move through this region to a region of stable burning very rapidly as the combustor pressure increased.

Flame radiation and headplate temperature. - Total flame radiation data were obtained at a single point in the combustor primary zone using a Leeds and Northrup radiometer. The radiometer was located 2.7 inches (6.86 cm) downstream of, and in line with, a fuel nozzle. The locations of thermocouples on the combustor headplate are shown in figure 18. Four thermocouples were used, two each near the inner and outer edges of the headplate, spaced 180° apart. Data were taken over a range of combustor operating conditions and with two sizes of fuel nozzles (number 1, high flow; number 2, lower flow (fig. 7)).

Figure 19 shows the variation in the measured radiant heat flux and headplate temperatures (average of the four thermocouples) with inlet-air pressure for both fuel nozzle sizes. The data were obtained with an undistorted inlet velocity profile at an inlet-air temperature of 600° F (589 K), a reference velocity of 150 feet per second (45.7 m/sec), and a fuel-air ratio of 0.022. The data show that the heat flux and headplate temperatures varied only slightly with pressure (for a given fuel nozzle) over the rather narrow test range.

The magnitude of the heat flux was about 3.5 times greater with the smaller-flow number 2 fuel nozzles (69 500 Btu/(ft<sup>2</sup>)(hr), 21.8 W/cm<sup>2</sup>) than with the larger-flow number 1 nozzles (20 000 Btu/(ft<sup>2</sup>)(hr), 6.0 W/cm<sup>2</sup>). A finer fuel spray occurs with the number 2 nozzles because of the larger pressure drop across the nozzles at the same fuel flow. The higher heat flux may indicate that the finer fuel spray from the number 2 nozzles moved the flame front closer to the radiometer viewing position. However, the headplate temperatures were not affected by the type of fuel nozzles and the resulting indicated change in heat flux. Heat flux and headplate temperature data were also obtained with distorted inlet-air velocity profiles but the differences, compared to the undistorted profile, were negligible.

Figure 20 shows the effects of fuel-air ratio and reference velocity on measured heat flux and headplate temperatures. The number 1 fuel nozzles were used, inlet-air conditions of 60 psia ( $41.4 \text{ N/cm}^2$ ) and  $1050^\circ \text{ F}$  ( $839 \text{ K}$ ) were held constant, and the velocity pressure profile was undistorted. The heat flux decreased and the headplate temperature increased as the fuel-air ratio was increased. The heat flux also decreased with increasing reference velocity. The headplate temperatures decreased slightly with increasing reference velocity.

Combustor exit temperature response to rapid increase in fuel flow. - Special tests were conducted to determine how well the combustor would react to a rapid increase in fuel flow. For these transient tests, a special 0.005-inch (0.127-mm) diameter, platinum-plus-13-percent-rhodium/platinum, wire thermocouple was mounted in the combustor exhaust plane. This thermocouple had a time constant of 0.0333 second. The measured temperatures were corrected for this time constant as well as for the radiation effects. The test conditions were 30-psia ( $20.6 \text{ N/cm}^2$ ) combustor pressure, 150-foot-per-second ( $45.7 \text{ m/sec}$ ) reference velocity, and  $600^\circ \text{ F}$  ( $589 \text{ K}$ ) inlet-air temperature. The test was started with the combustor operating at a fuel flow rate of 0.355 pound per second ( $0.161 \text{ kg/sec}$ ), giving an initial temperature rise of  $590^\circ \text{ F}$  ( $328 \text{ K}$ ). A step increase in fuel flow was then made to produce a theoretical temperature rise of about  $1300^\circ \text{ F}$  ( $722 \text{ K}$ ) in 0.9 second.

The ratio of instantaneous temperature rise (temperature rise after start of increase of fuel flow) to initial temperature rise (temperature rise at start of increase of fuel flow)  $\Delta T_t / \Delta T_o$  is plotted against time from start of increase of fuel flow in figure 21. Also plotted against time in this figure is the ratio of instantaneous fuel flow to initial fuel flow  $\dot{w}_t / \dot{w}_o$ . A third curve on this figure is the exit temperature rise at the location of the fast-response thermocouple measured during steady-state operation at various fuel flow rates. The steady-state data were obtained at 100 percent combustion efficiency.

For conditions of constant combustion efficiency and stable exhaust temperature pattern, the ratio  $\Delta T_t / \Delta T_o$  will very nearly equal  $\dot{w}_t / \dot{w}_o$  because of the nearly linear relation of ideal exit temperature to fuel flow. The amount of nonlinearity is seen in figure 21 between the steady-state curve (which is also the ideal temperature because of 100 percent combustion efficiency) and the fuel flow ratio curve  $\dot{w}_t / \dot{w}_o$ .

The data of figure 21 show the combustor to have very good temperature response. The temperature increased almost as rapidly as the fuel flow increased, starting with an apparent immediate response. After about 0.5 second, the temperature rise had caught up with the rapid change in fuel flow. Comparing the temperature rise curve with the steady-state curve indicates a high combustion efficiency during the transient condition. Further tests at inlet-air temperatures as low as  $250^\circ \text{ F}$  ( $394 \text{ K}$ ) produced similar results of which these curves are typical.

Smoke density evaluations. - Measurements were made to determine the general level of smoke density in the combustor exhaust gases at several operating conditions.

Table V lists the smoke number (defined in appendix B) obtained at the various operating conditions. Smoke numbers obtained at conditions simulating Mach 2.7 and 3.0 cruise were very low, below the threshold of visible smoke. However, the smoking characteristics at the takeoff condition are of more interest: 180-psia ( $124\text{-N/cm}^2$ ) inlet-air total pressure,  $600^\circ\text{ F}$  ( $589\text{ K}$ ) inlet-air temperature, and 100-feet-per-second ( $30.5\text{-m/sec}$ ) reference velocity. Since the facility could not provide a pressure of 180 psia ( $124\text{ N/cm}^2$ ), the smoke number for that condition ( $124\text{ N/cm}^2$ ) was extrapolated from data in reference 5. Using data obtained at a combustor pressure of 90 psia ( $62.0\text{ N/cm}^2$ ), the smoke number at takeoff was extrapolated to have a value of 36. This value is in the range of lightly visible smoke.

## SUMMARY OF RESULTS

A full-scale ram-induction annular combustor designed for Mach 3 cruise conditions was tested at Lewis Research Center for endurance and performance. The following results were obtained:

1. Combustor endurance was determined for 325 hours of cyclic operation at inlet-air temperatures to  $1150^\circ\text{ F}$  ( $894\text{ K}$ ), pressures to 90 psia ( $62.0\text{ N/cm}^2$ ), and an average exit temperature of  $2200^\circ\text{ F}$  ( $1478\text{ K}$ ). The combustor sustained burned scoops, burned areas on inner liner surfaces, and thermal stress cracks. However, the combustion efficiency, total pressure loss, exit temperature profile, and pattern factor were not affected by the physical deterioration of the combustor.

2. Combustion efficiencies were 100 percent for inlet operating conditions where pressures were greater than 30 psia ( $20.6\text{ N/cm}^2$ ), temperatures were above  $600^\circ\text{ F}$  ( $589\text{ K}$ ), and reference velocities were 100 to 200 feet per second ( $30.5$  to  $61.0\text{ m/sec}$ ). Efficiency dropped at pressures below 30 psia ( $20.6\text{ N/cm}^2$ ) to an approximate value of 85 percent at 5 psia ( $3.4\text{ N/cm}^2$ ). Efficiency also decreased with decreasing inlet-air temperatures. A combustion efficiency of 60 percent was measured at an inlet-air temperature of  $100^\circ\text{ F}$  ( $311\text{ K}$ ).

3. The combustor total pressure loss, which includes the diffuser loss, was affected by diffuser inlet velocity profile. At the Mach 2.7 cruise condition ( $1050^\circ\text{ F}$  ( $839\text{ K}$ ) and 60 psia ( $41.4\text{ N/cm}^2$ )) and with a uniform inlet velocity profile, the total pressure loss was 5.6 percent. The total pressure loss increased when the diffuser inlet velocity profile was distorted to simulate the profile measured in engine tests. At the Mach 2.7 cruise condition, the isothermal total pressure loss increased to 6.9 percent. At the



Mach 3.0 cruise condition of the endurance evaluation, the pressure loss with combustion measured 7.4 percent with the distorted profile.

4. The exit radial average temperature profile was in good agreement, with the design average profile, not exceeding it by more than  $60^{\circ}\text{ F}$  ( $33\text{ K}$ ) for the Mach 3 cruise and simulated takeoff conditions. The temperature profile was generally insensitive to changes to the diffuser inlet velocity profile, showing only about  $75^{\circ}\text{ F}$  ( $42\text{ K}$ ) deviation. A change from a uniform velocity pressure profile to one distorted toward the outer diameter caused the inner annulus airflow to decrease from 38 to 22 percent of total flow. With this large airflow change, the exit temperature near the hub increased only about  $60^{\circ}\text{ F}$  ( $33\text{ K}$ ).

5. Exit temperature profile parameters obtained over many hours of testing were quite satisfactory. For simulated takeoff conditions, the average values of pattern factor  $\bar{\delta}$ ,  $\delta_{\text{stator}}$ , and  $\delta_{\text{rotor}}$  were 0.29, 0.20, and 0.085, respectively. For Mach 3 cruise conditions, the average values were 0.19, 0.14, and 0.064, respectively.

6. Combustor relight limits at low inlet-air pressures and temperatures were 5.0 psia ( $3.4\text{ N/cm}^2$ ) at  $300^{\circ}\text{ F}$  ( $422\text{ K}$ ) and 8 psia ( $5.5\text{ N/cm}^2$ ) at  $90^{\circ}\text{ F}$  ( $300\text{ K}$ ) at a reference Mach number of 0.1 and a fuel-air ratio of 0.01. The minimum pressure for relight increased sharply at temperatures near  $65^{\circ}\text{ F}$  ( $292\text{ K}$ ). Combustion was maintained below the relight limits. Only one blowout point (5 psia ( $3.4\text{ N/cm}^2$ ) at  $75^{\circ}\text{ F}$  ( $297\text{ K}$ )) occurred within the limits of the test facility.

7. For a fixed fuel nozzle size and fuel-air ratio, the measured heat flux and head-plate temperatures varied only slightly with inlet-air pressure. Smaller fuel-flow nozzles increased the heat flux by a factor of 3 without changing the headplate temperatures. Heat flux decreased with increasing fuel-air ratio and reference velocity.

8. Combustor exit temperature response to a rapid step increase in fuel-air ratio was very good. The temperature increased almost as rapidly as the fuel flow during the 0.9 second when the temperature rise was increased to about  $1300^{\circ}\text{ F}$  ( $722\text{ K}$ ). High combustion efficiency was maintained during the transient condition.

9. Exhaust gas smoke numbers obtained to evaluate smoke density varied from measured values below the threshold of visible smoke at cruise conditions, to extrapolated values indicating lightly visible smoke at simulated takeoff conditions.

Lewis Research Center,  
National Aeronautics and Space Administration,  
Cleveland, Ohio, June 9, 1970,  
720-03.

## APPENDIX A

### TEST FACILITY

The full-scale advanced annular combustor investigation was conducted in a closed-duct test facility of the Engine Components Research Laboratory of the Lewis Research Center. A sketch of this facility is shown in figure 22. Airflows for combustion up to 300 pounds per second (136 kg/sec) at pressures from below atmospheric to 10 atmospheres could be heated to 1200<sup>0</sup> F (922 K) without vitiation before entering the combustor under test.

Figure 23 shows the combustor test section and the connected inlet and outlet ducting. About  $4\frac{1}{2}$  pipe diameters of constant-area duct was ahead of the test section. Following the inlet ducting was the combustor housing, which included the diffuser inlet and diffuser as part of the housing. The combustor housing measured 42 inches (1.07 m) at the maximum diameter by 37.75 inches (0.96 m) long. Following the combustor housing was the outlet instrumentation section. At this section and downstream, the combustor exhaust gases were cooled by a water injection spray system. The exposed surfaces downstream of the combustor were cooled by two methods: (1) circulating water in passages adjacent to the hot surfaces, and (2) water sprays impinging directly on the exposed surfaces. The test section installation is shown in figure 24.

For combustor inlet temperatures of 600<sup>0</sup> F (589 K) or less, an indirect-fired heat exchanger was used. For higher inlet temperatures (to 1200<sup>0</sup> F , 922 K), a second stage of indirect heating was used. Heat for the second stage was provided by a natural-gas-fueled J-57 jet engine with an afterburner. The engine exhaust gases were passed through a heat exchanger of special design shown in figure 25.

Airflow rates and combustor pressures were regulated by remotely controlled valves upstream and downstream of the test section. Flow straighteners were used to evenly distribute the airflow entering the combustor (see fig. 22).

## APPENDIX B

### INSTRUMENTATION

Measurements to determine combustor operation and performance were recorded by the Center's Central Automatic Data Processing System (ref. 6). Control room readout instrumentation (indicating and recording) was used to set and monitor the test conditions and the operation of the combustor. Pressures were measured and recorded by the central Digital Automatic Multiple Pressure Recorder (DAMPR) and by strain-gage-type pressure transducers (ref. 7). Temperatures were measured by iron-constantan and Chromel-Alumel thermocouples for low- and medium-temperature conditions and by platinum/platinum-plus-13-percent-rhodium thermocouples for high temperatures. The indicated readings of all thermocouples were taken as true values of the total temperatures. The platinum-plus-13-percent-rhodium/platinum thermocouples were of the high-recovery aspirating type (ref. 8, type 6).

Airflow rates were measured by square-edged orifices installed according to ASME specifications. Fuel flow rates were measured by turbine-type flowmeters using frequency-to-voltage converters for readout and recording.

The locations of the combustor instrumentation stations axially along the test section are shown in figure 23. Instrumentation at inlet station 3 is shown in figure 26. Inlet-air temperature was measured by eight Chromel-Alumel thermocouples located at equal spacing around the inlet at station 3. Inlet-air total pressure was measured by eight five-point total pressure rakes equally spaced around the inlet at station 3. The pressure rakes measured the total pressure profile at centers of equal areas across the inlet annulus. Static pressure at the inlet was measured by 16 wall static pressure taps with eight on the outside and eight on the inside walls of the annulus.

Airflow in the combustor inner and outer flow passages was calculated from four total pressure tubes and one streamline static pressure tube in each of the inner and outer passages. One total pressure tube and one wall static pressure tap were used in the center passage. Location of this instrumentation is shown in figure 27.

Combustor outlet total temperature and pressure at instrumentation station 5 were measured at  $3^{\circ}$  increments around the exit circumference (see fig. 3). At each  $3^{\circ}$  increment, five temperature and pressure points were measured across the annulus. These points were located at centers of equal areas across the annulus. The water-cooled probe assembly containing the five temperature and pressure sensors is shown in figure 28. Three of these probes, each on an arm  $120^{\circ}$  apart, rotated  $120^{\circ}$  providing full coverage of the circumference. Water-cooled shields protected these probes when not in use at three fixed points in the exhaust stream. At these points, temperature and

pressure were not measured. The probes were made of platinum-rhodium alloy where exposed to the hot exhaust gases. Also located at station 5 were eight wall static pressure taps.

A schematic of the equipment used to obtain the smoke density, or smoke number (SN), is shown in figure 29. Combustor exhaust gas samples were picked up by the aspirating thermocouple probes and cooled to room temperature by a heat exchanger. A portion of these gases, which was used to obtain the smoke number, was piped into a plenum chamber. The chamber was continuously purged by these gases and maintained at about 2-psi ( $1.4 \text{ N/cm}^2$ ) pressure above atmospheric pressure. A Von Brand smoke-meter was used to obtain the smoke stain on Whatman number 4 filter tape. To obtain a smoke stain, the vacuum pump was started and the gas flow adjusted to 0.6 standard cubic foot per minute ( $2.83 \times 10^{-4} \text{ m}^3/\text{sec}$ ) as measured by the calibrated rotameter. A pressure drop across the filter tape of about 5 inches of mercury ( $1.7 \text{ N/cm}^2$ ) was maintained for all the tests. The tape speed was 4 inches per minute ( $0.17 \text{ cm/sec}$ ), which gave a sample flow rate of 0.3 standard cubic foot per minute per square inch ( $2.19 \times 10^{-5} \text{ m}^3/(\text{sec})(\text{cm}^2)$ ) of tape. Two moisture traps were used between the plenum chamber and the heated head on the smoke meter. During a test, some moisture was carried into the first trap; however, none was ever evident in the second trap.

The absolute reflectivity of the stained filter tape was measured with a Welsh Densichron using a gray background. The Densichron was calibrated with a Welsh Gray Scale.

The smoke number was determined from the following equation:

$$\text{SN} = 100 \left( 1 - \frac{\text{Percent absolute reflectivity of sample}}{\text{Percent absolute reflectivity of clean paper}} \right)$$

## REFERENCES

1. Chamberlain, John: The Ram-Induction Combustor Concept. Presented at the AIAA Third Propulsion Joint Specialist Conference, Washington, D. C. , July 17-21, 1967.
2. Rusnak, J. P. ; and Shadowen, J. H. : Development of an Advanced Annular Combustor. Rep. PWA-FR-2832, Pratt & Whitney Aircraft. (NASA CR-72453), May 30, 1969.
3. Butze, Helmut F. ; Trout, Arthur M. ; and Moyer, Harry M. : Performance of Swirl-Can Turbojet Combustors at Simulated Supersonic Combustor-Inlet Conditions. NASA TN D-4996, 1969.
4. Humenik, Francis M. : Performance of a Short-Length Turbojet Combustor Insensitive to Radial Distortion of Inlet Airflow. NASA TN D-5570, 1970.
5. Bagnetto, Lucien: Smoke Abatement in Gas Turbines. Part II: Effects of Fuels, Additives and Operating Conditions on Smoke Emissions and Flame Radiation. Rep. 5127-68-Pt. 2, Phillips Petroleum Co. , Sept. 1968. (Available from DDC as AD-842818.)
6. Mealey, Charles; and Kee, Leslie: A Computer-Controlled Central Digital Data Acquisition System. NASA TN D-3904, 1967.
7. Staff of the Lewis Laboratory: Central Automatic Data Processing System. NACA TN 4212, 1958.
8. Glawe, George E. ; Simmons, Frederick S. ; and Stickney, Truman M. : Radiation and Recovery Corrections and Time Constants of Several Chromel-Alumel Thermocouple Probes in High-Temperature, High-Velocity Gas Streams. NACA TN 3766, 1956.

TABLE I. - RAM-INDUCTION COMBUSTOR  
DIMENSIONS AND SPECIFICATIONS

Length, in. (cm):	
Compressor exit to turbine inlet	30.20 (76.7)
Fuel nozzle face to turbine inlet	20.68 (52.53)
Diameter, in. (cm):	
Inlet outside	31.80 (80.77)
Inlet inside	28.00 (71.1)
Outlet outside	35.38 (89.9)
Outlet inside	27.50 (69.9)
Shroud outside	37.09 (94.2)
Shroud inside	22.52 (57.2)
Combustor liner volume, ft <sup>3</sup> (m <sup>3</sup> )	5.02 (0.142)
Reference area (between shrouds), in. <sup>2</sup> (cm <sup>2</sup> )	695 (4484)
Diffuser inlet area, in. <sup>2</sup> (cm <sup>2</sup> )	182.5 (1177)
Open hole area (including cooling, in. <sup>2</sup> (cm <sup>2</sup> ):	
Model A	352 (2271)
Model F	289 (1865)
Snout inlet area, in. <sup>2</sup> (cm <sup>2</sup> )	61.5 (397)
Exit area, in. <sup>2</sup> (cm <sup>2</sup> )	388 (2503)
Number of fuel nozzles and swirlers	24
Number of diffuser struts	12
Number of ram-induction scoops	240
Rows, primary zone	3
Rows, secondary zone	2
Ratio length to annulus height	2.9

TABLE II. - COMBUSTOR ENDURANCE TEST CONDITIONS, OPERATING  
TIME, AND PERFORMANCE - MODEL F

Test	Condition	Inlet-air conditions						Combustor Conditions				Operating time, hr
		Pressure		Temper- ature		Flow		Outlet temper- ature		Reference velocity		
		psia	N/cm <sup>2</sup>	°F	K	lb/sec	kg/sec	°F	K	ft/sec	m/sec	
1	Mach 2.7 cruise	60	41.4	1050	839	77.4	35.1	1900	1311	150	45.7	35
2	Mach 2.7 cruise	60	41.4	1050	839	72.3	32.8	2200	1478	140	42.7	100
3	Mach 3.0 cruise	90	62.0	1150	895	116.3	52.8	1900	1311	160	48.8	30
4	Mach 3.0 cruise	↓	↓	1150	895	108.6	49.3	2200	1478	150	45.7	150
5	Simulated takeoff	↓	↓	600	589	117.8	53.4	1900	1311	108	32.9	5
6	Simulated takeoff	↓	↓	600	589	110.3	50.0	2200	1478	100	30.5	5

Test	Condition	Combustor performance				
		Efficiency, percent	Total pressure loss, percent	Exit temperature profile parameters		
				Pattern factor, $\frac{\delta}{\bar{\delta}}$	$\delta_{\text{stator}}$	$\delta_{\text{rotor}}$
1	Mach 2.7 cruise	100	7.6	0.18 to 0.19	0.13	0.045
2	Mach 2.7 cruise	↓	7.4	.17 to 0.20	.16	.054
3	Mach 3.0 cruise	↓	8.1	.19 to 0.22	.16	.051
4	Mach 3.0 cruise	↓	7.4	.18 to 0.24	.14	.064
5	Simulated takeoff	↓	5.5	.21 to 0.25	.13	.081
6	Simulated takeoff	↓	5.2	.24 to 0.30	.20	.085

TABLE III. - EXPERIMENTAL DATA

Combustor inlet conditions										Combustor operation results																			
Total pressure		Total temperature		Airflow		Reference velocity		Diffuser inlet Mach number	Diffuser inlet velocity pressure profile <sup>a</sup>	Fuel nozzle size	Fuel-air ratio	Fuel nozzle pressure differential		Average exhaust temperature		Combustion efficiency, percent	Total pressure loss, percent	Pattern factor, $\bar{\delta}$	Average radial temperature		Maximum local radial temperature	Maximum circumferential average temperature	Flame radiation		Headplate temperature		Smoke number		
psia	N/cm <sup>2</sup>	°F	K	lb/sec	kg/sec	ft/sec	m/sec					psid	N/cm <sup>2</sup> d	°F	K				°F	K			°F	K	Btu (ft <sup>2</sup> )(hr)	W/cm <sup>2</sup>		°F	K
61.4	42.3	615	597	110.5	22.7	147	44.8	0.404	OD	1	0.0226	432	298	2039	1388	101.5	10.01	0.231				2253	1507	20.3×10 <sup>3</sup>	6.4	780	689	<1	
51.6	35.6	602	590	92.5	42.0	145	44.2	.397			.0224	295	203	2030	1383	102.7	9.07	.209				2214	1485					2.0	
40.8	28.1	597	587	75.9	34.4	149	45.4	.414			.0218	189	130	1993	1363	102.6	8.87	.174				2183	1468					<1	
30.6	21.1	605	591	56.9	27.2	150	45.7	.418			.0218	105	72	1981	1356	101.3	9.50	.168				2143	1446					<1	
40.4	27.9	602	590	73.8	33.5	148	45.1	.397	U	2	.0226	736	507	2061	1375	100.8	9.74	.360				2339	1555					650	
39.8	27.4	608	593	72.2	32.7	148	45.1	.398			.0199	472	325	1879	1299	101.6	10.19	.363				2023	1379					750	
30.0	20.7	598	588	53.7	24.4	145	44.2	.387			.0199	252	174	1858	1288	100.8	9.07	.330				2106	1425					740	
30.6	21.1	595	586	56.7	25.7	149	45.4	.404			.0215	332	229	1963	1346	102.0	10.70	.361				2246	1503					655	
30.6	21.1	603	590	55.1	25.0	146	44.5	.392			.0225	394	272	1993	1363	99.4	10.17	.353				2292	1529	70.5	22.2			655	
25.6	17.7	598	588	45.0	20.4	142	43.3	.381			.0229	268	185	2005	1369	98.9	9.61	.315				2275	1519	70.5	22.2			630	
25.3	17.4	593	585	46.8	21.2	148	45.1	.402			.0193	178	123	1823	1268	100.8	10.13	.302				2053	1396					670	
20.3	14.0	589	583	38.1	17.3	150	45.7	.409			.0189	114	79	1793	1251	100.4	10.02	.269				2026	1381					660	
20.5	14.1	597	587	36.8	16.7	145	44.2	.389			.0226	174	120	1980	1355	98.3	9.52	.262				2186	1470						
19.6	13.5	597	587	35.7	16.2	146	44.5	.393			.0232	164	113	2015	1375	98.8	8.95	.264				2230	1494	69.8	22.0			634	
14.8	10.2	592	584	26.9	12.2	146	44.5	.393			.0229	90	62	1968	1349	96.9	9.67	.270				2185	1469	69.8	22.0			638	
15.1	10.4	598	588	27.9	12.7	149	45.4	.405			.0223	95	66	1935	1330	96.4	9.32	.266				2133	1440						
15.0	10.3	583	579	28.1	12.7	149	45.4	.406			.0216	83	57	1914	1319	98.4	8.89	.260				2116	1431					630	
10.1	7.0	592	584	18.9	8.6	150	45.7	.408			.0220	43	30	1884	1302	94.3	9.40	.281				2101	1423						
10.4	7.2	591	584	18.5	8.4	142	43.3	.380			.0222	39	27	1849	1283	91.1	7.44	.271				2034	1385	69.8	22.0			652	
20.7	14.3	590	583	37.4	17.0	144	43.9	.398	OD	3	.0140	910	627	1483	1079	98.4	10.99	.218				1615	1153					710	
15.6	10.8	596	586	28.9	13.1	148	45.1	.415			.0183	919	634	1719	1210	96.7	11.16	.205				1866	1292					665	
15.6	10.8	591	584	27.9	12.7	143	43.6	.397			.0190	918	633	1747	1226	96.0	10.67	.223				1903	1313					655	
10.3	7.1	590	583	19.1	8.7	147	44.8	.415			.0196	437	301	1746	1225	93.3	12.53	.229				1877	1298					645	
10.3	7.1	588	582	19.4	8.8	150	45.7	.425			.0193	437	301	1736	1220	94.1	11.61	.225				1876	1298					645	
8.3	5.7	574	574	15.4	7.0	146	44.5	.412			.0198	279	192	1720	1211	91.7	10.32	.231				1875	1297					630	
8.3	5.7	570	572	15.3	6.9	143	43.6	.408			.0228	377	260	1881	1300	92.1	9.63	.211				2050	1394					620	
4.9	3.4	569	571	7.3	3.3	117	35.7	.313			.0263	106	73	1895	1308	82.2	1.89	.285				2110	1428					620	
5.2	3.6	516	542	8.6	3.9	124	37.8	.351			.0228	109	75	1719	1210	84.1	6.15	.235				1882	1301					590	
5.3	3.7	565	569	9.6	4.4	141	43.0	.404			.0202	105	72	1628	1160	83.0	7.83	.262				1772	1240					615	
5.3	3.7	559	566	10.2	4.6	148	45.1	.425			.0221	142	98	1776	1242	87.9	6.38	.241				1923	1324					605	
29.6	20.4	89	305	105.8	48.0	145	44.2	.657	U	1	.0119	97	67	580	578	57.7	21.0												
29.8	20.5	594	585	58.9	26.7	158	48.2	.440			.0142	44	30	1499	1088	97.5	11.18												
29.8	20.5	595	586	58.8	26.7	158	48.2	.439			.0210	94	65	1907	1315	99.0	11.61												





TABLE III. - Concluded. EXPERIMENTAL DATA

[illegible]

59.3	40.9	597	587	115.5	52.4	157	47.9	.428	U	.0217	441	304	1987	1359	102.7	9.68	.379	-----	2361	1567	22.0	7.0	680	633	1.2
49.8	34.3	600	589	96.6	43.8	157	47.9	.423		.0214	301	208	1992	1362	104.1	9.28	.299	-----	2278	1521	20.5	6.5	680	633	---
39.5	27.2	603	590	79.1	35.9	162	49.4	.443		.0208	190	131	1949	1338	103.1	9.86	.351	-----	2273	1518	20.0	6.3	670	628	1.9
29.9	20.6	604	591	53.7	24.4	145	44.2	.398		.0230	106	73	1940	1333	93.7	9.18	.327	-----	2248	1504	20.0	6.3	630	605	---
19.8	13.7	614	596	34.0	15.4	140	42.7	.389		.0244	48	33	1839	1277	81.5	7.89	.291	-----	2088	1415	18.5	5.8	650	684	---
24.9	17.2	601	589	43.9	19.9	142	43.3	.381	2	.0238	268	185	2069	1405	99.9	8.82	.274	-----	2333	1551	69.8	22.0	637	609	---
19.6	13.5	597	587	35.7	16.2	146	44.5	.393		.0232	164	113	2015	1375	98.8	8.95	.264	-----	2230	1494			634	608	---
14.8	10.2	592	584	26.9	12.2	146	44.5	.393		.0229	90	62	1968	1349	96.9	9.67	.270	-----	2185	1469			638	610	---
10.4	7.2	591	584	18.5	8.4	142	43.3	.380		.0222	39	27	1849	1283	91.1	7.44	.271	-----	2034	1385			652	618	---
7.4	5.1	579	577	10.0	4.5	107	32.6	.280		.0197	12	8	1293	974	57.3	3.80	.498	-----	1443	1057			665	625	---
57.3	39.5	1055	841	66.6	30.2	131	39.9	.278	1	.0119	46	22	1806	1259	102.6	3.22	.171	-----	1886	1303	69.9	22.1	1365	1014	1.3
59.5	41.0	1055	841	65.3	29.6	128	39.0	.272		.0151	71	49	1970	1350	100.2	3.58	.205	-----	2086	1414	66.9	20.4	1335	997	---
59.7	41.1	1058	843	64.7	29.3	126	38.4	.270		.0207	128	88	2287	1526	100.4	3.92	.223	-----	2456	1620	51.2	16.1	1450	1061	---
58.7	40.5	1052	840	77.5	35.2	153	46.6	.336		.0126	70	48	1810	1261	97.9	4.96	.211	-----	1913	1318	52.6	16.6	1335	997	<1
59.9	41.3	1051	839	80.2	36.4	155	47.2	.342		.0148	101	70	1962	1345	101.5	6.79	.185	-----	2062	1401	49.6	15.7	1365	1014	---
59.9	41.3	1051	839	76.7	34.8	148	45.1	.327		.0191	154	106	2154	1452	96.8	6.08	.225	-----	2299	1533	44.7	14.1	1395	1030	4.5
59.2	40.8	1053	840	78.6	35.7	154	46.9	.338		.0206	187	129	2274	1519	100.0	5.59	.218	-----	2432	1606	42.3	13.4	1400	1033	---
59.1	40.7	1056	842	94.1	42.7	184	56.1	.421		.0120	93	64	1806	1259	101.8	8.66	.204	-----	1901	1311	43.7	13.8	1330	994	1.5
59.2	40.8	1056	842	94.1	42.7	184	56.1	.421		.0147	137	94	1962	1345	101.4	8.98	.204	-----	2079	1410	41.8	13.1	1365	1014	1.5
58.7	40.5	1053	840	93.8	42.5	184	56.1	.423		.0181	203	140	2150	1450	101.4	8.61	.219	-----	2299	1533	38.4	12.1	1375	1019	---
59.1	40.7	1047	837	94.1	42.7	183	55.8	.420		.0201	254	175	2260	1511	101.7	9.14	.232	-----	2436	1609	37.0	11.7	1370	1016	3.0
59.5	41.0	1055	841	101.7	46.1	197	60.0	.465		.0133	127	88	1872	1295	100.8	11.18	.224	-----	1990	1361	39.0	12.3	1480	1078	1.6
59.3	40.9	1052	840	100.6	45.6	195	59.4	.459		.0162	185	128	2034	1385	100.1	10.49	.233	-----	2165	1458	36.5	11.5	1635	1164	---
58.9	40.6	1057	843	103.2	46.8	202	61.6	.478		.0185	252	174	2178	1465	101.4	10.48	.247	-----	2348	1560	35.6	11.2	1650	1172	---
59.1	40.7	1049	838	102.3	46.4	199	60.7	.469		.0204	300	207	2265	1514	100.7	10.74	.256	-----	2464	1624	34.8	11.0	1625	1158	2.8
60.9	42.0	1052	840	76.5	34.7	145	44.2	.324	OD	.0125	65	31	1839	1277	102.3	7.74	.202	-----	1921	1323	-----	---	1295	975	<1
61.1	42.1	1049	838	76.7	34.8	145	44.2	.319		.0153	96	66	1999	1366	102.3	7.65	.201	-----	2087	1415	-----	---	1320	989	1.0
61.3	42.3	1050	839	75.7	34.3	143	43.6	.316		.0198	154	106	2240	1500	101.3	8.20	.227	-----	2383	1579	-----	---	1380	1022	<1
91.1	62.8	1154	896	104.6	47.4	142	43.3	.301		.0177	237	163	2216	1486	101.1	5.48	.197	-----	2339	1555	89.0	28.0	1530	1105	<1
90.3	62.3	605	591	115.3	52.3	104	31.7	.262	U	.0211	420	290	1952	1340	102.2	5.46	.401	-----	2280	1522	-----	---	930	772	17.0
29.3	20.2	312	429	31.5	14.3	64	19.5	.204	OD	-----	---	---	301	423	-----	2.94	-----	-----	-----	-----	-----	-----	-----	-----	-----
29.3	20.2	319	433	66.9	30.3	135	41.1	.489	OD	-----	---	---	308	426	-----	11.50	-----	-----	-----	-----	-----	-----	-----	-----	-----
29.0	20.0	308	426	85.3	38.7	167	50.9	.735	OD	-----	---	---	300	422	-----	23.50	-----	-----	-----	-----	-----	-----	-----	-----	-----
29.5	20.3	302	423	31.4	14.2	62	18.9	.189	U	-----	---	---	291	417	-----	2.27	-----	-----	-----	-----	-----	-----	-----	-----	-----
29.6	20.4	303	424	69.0	31.3	135	41.1	.463	U	-----	---	---	296	420	-----	10.93	-----	-----	-----	-----	-----	-----	-----	-----	-----
29.4	20.3	312	429	89.6	40.6	174	53.0	.738	U	-----	---	---	303	424	-----	22.02	-----	-----	-----	-----	-----	-----	-----	-----	-----
29.8	20.5	297	420	31.0	14.1	61	18.6	.188	ID	-----	---	---	285	414	-----	2.27	-----	-----	-----	-----	-----	-----	-----	-----	-----
29.6	20.4	299	421	66.9	30.3	130	39.6	.448	ID	-----	---	---	290	416	-----	10.58	-----	-----	-----	-----	-----	-----	-----	-----	-----
30.1	20.8	307	426	85.5	38.8	162	49.4	.656	ID	-----	---	---	297	420	-----	19.87	-----	-----	-----	-----	-----	-----	-----	-----	-----

<sup>a</sup>U Diffuser inlet velocity pressure profile; uniform, nondistorted, or flat.

OD Distorted toward outer diameter.

ID Distorted toward inner diameter.

UOD Unsymmetrically distorted toward outer diameter.

TABLE IV. - EFFECT OF AIR VELOCITY PROFILE  
ON COMBUSTOR PASSAGE AIRFLOW

Velocity profile	Percent of total air-flow in flow passages		
	Inner	Center (snout)	Outer
Uniform	36	28	36
Distorted toward outside diameter	22	35.5	42.5
Distorted toward inside diameter	34	32.5	33.5

TABLE V. - MEASURED SMOKE NUMBER

Smoke number	Design condition	Nominal inlet conditions						Nominal combustor average exhaust temperature	
		Total pressure		Total temperature		Reference velocity		°F	K
		psia	N/cm <sup>2</sup>	°F	K	ft/sec	m/sec		
<1	-----	60	41.4	1050	839	150	45.7	1800	1256
<1	-----	60	41.4	1050	839	↓	↓	2000	1367
<1	Mach 2.7 cruise	60	41.4	1050	839	↓	↓	2200	1478
<1	Mach 3.0 cruise	90	62.0	1150	895	↓	↓	2200	1478
17	-----	90	62.0	600	589	100	30.5	2000	1367
<sup>a</sup> 36	Simulated takeoff	<sup>a</sup> 180	124.1	600	589	100	30.5	2000	1367

<sup>a</sup>Extrapolated.

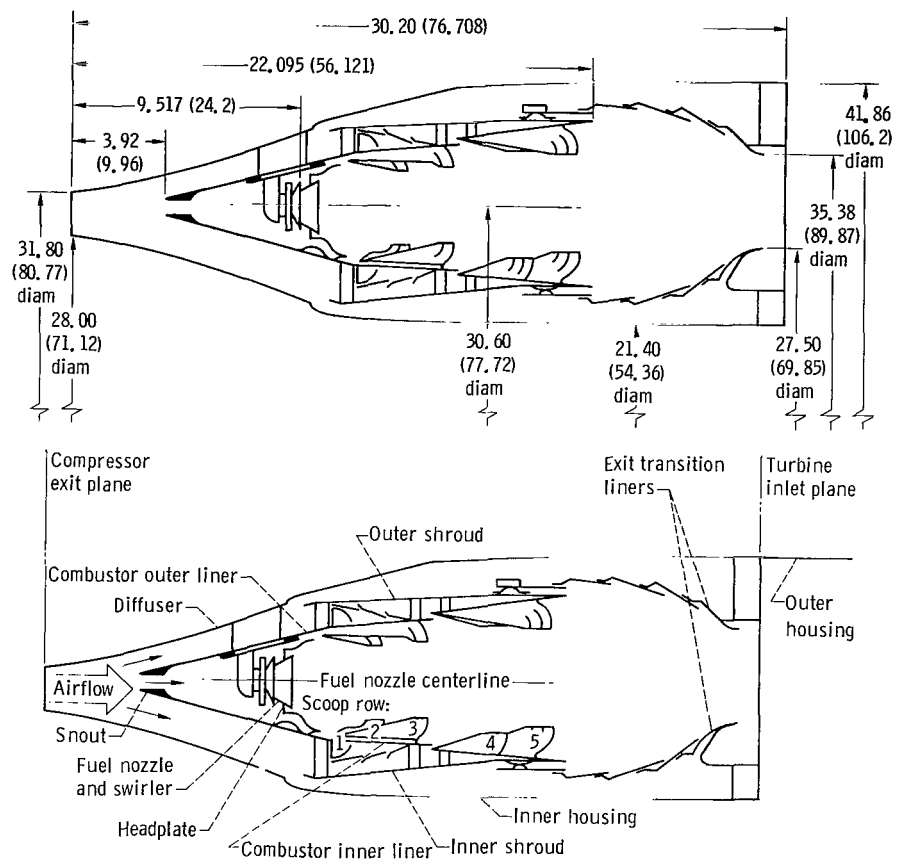
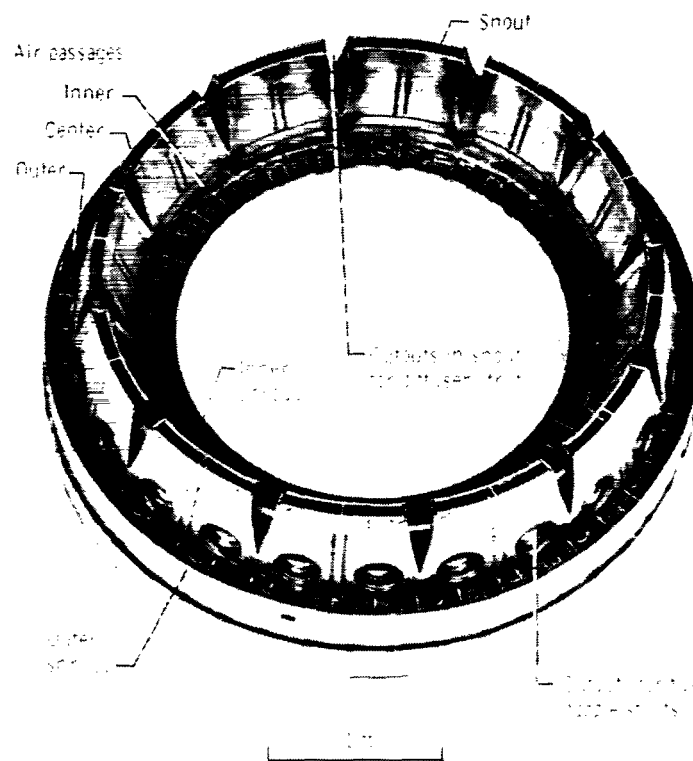
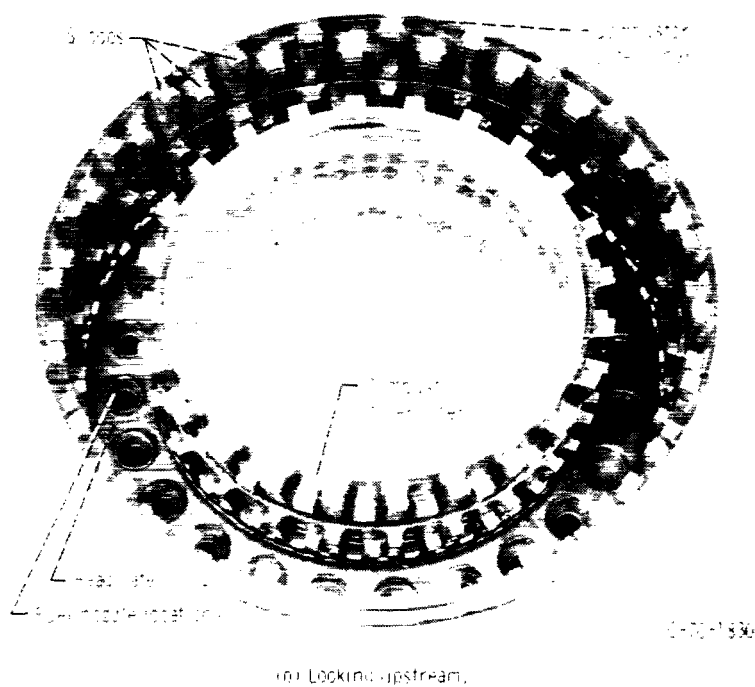


Figure 1. - Cross-section sketch of modified JTF-17 ram-induction annular combustor. (Dimensions are in inches (cm).)

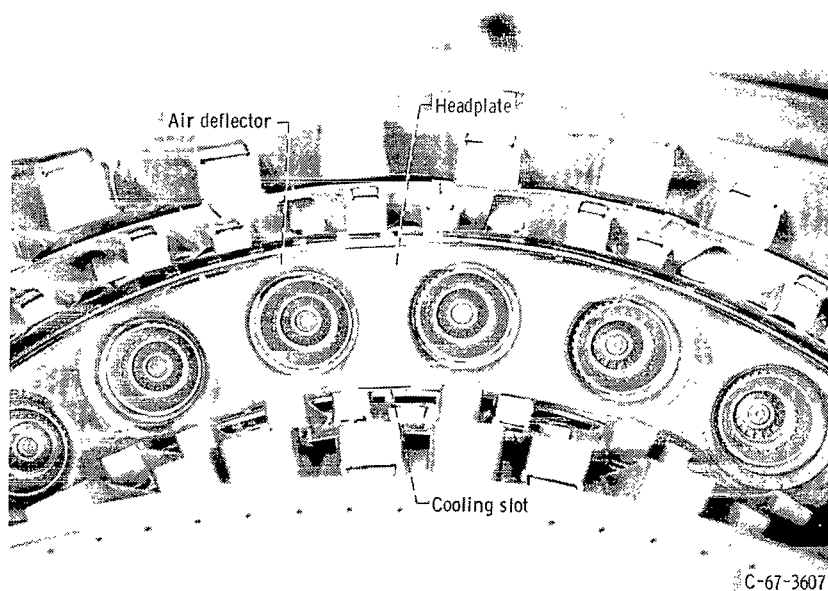


(a) Looking downstream.



(b) Looking upstream.

Figure 2. - Annular ram-induction combustor.



(c) Closeup view looking upstream.  
Figure 2. - Concluded.

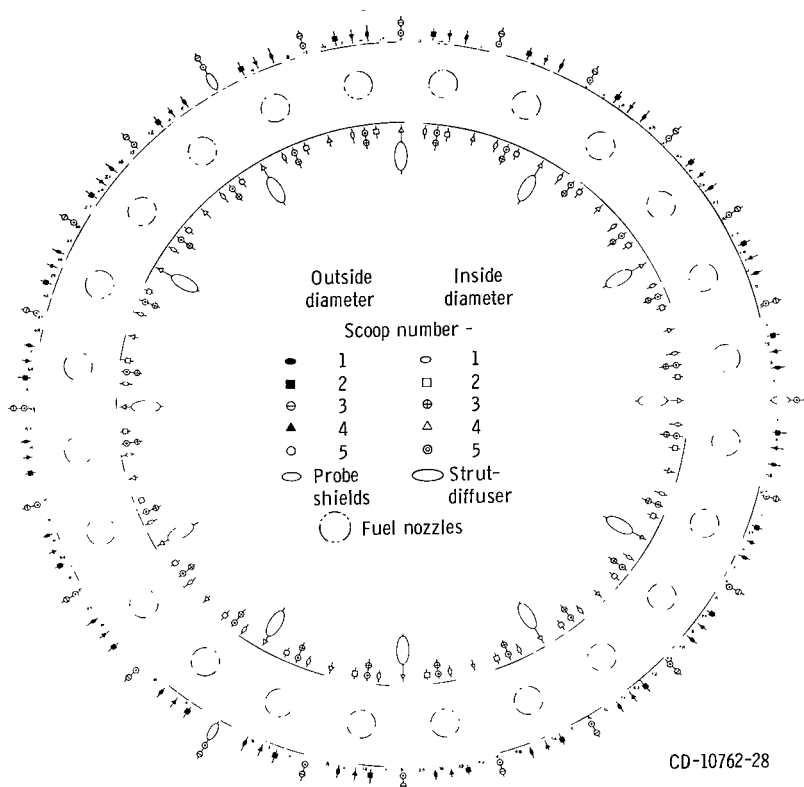


Figure 3. - Circumferential locations of scoops, fuel nozzles, diffuser struts, exit temperature measuring points, and probe shields. View looking upstream. Numbers 3 to 117 denote exit temperature measuring points.

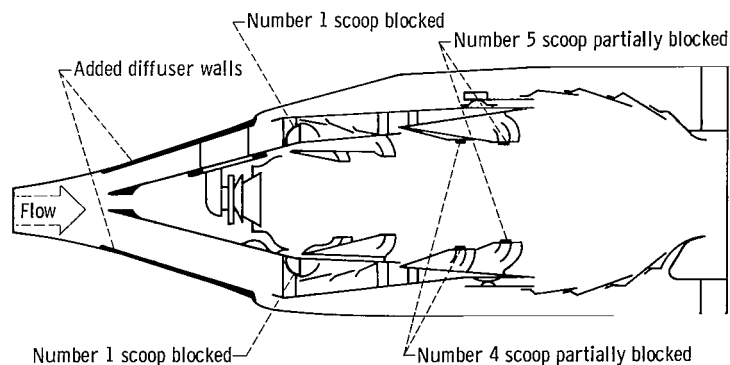
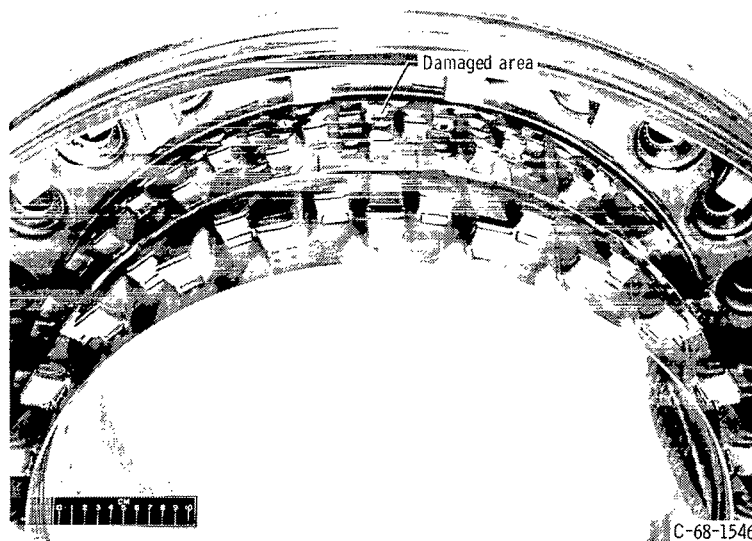
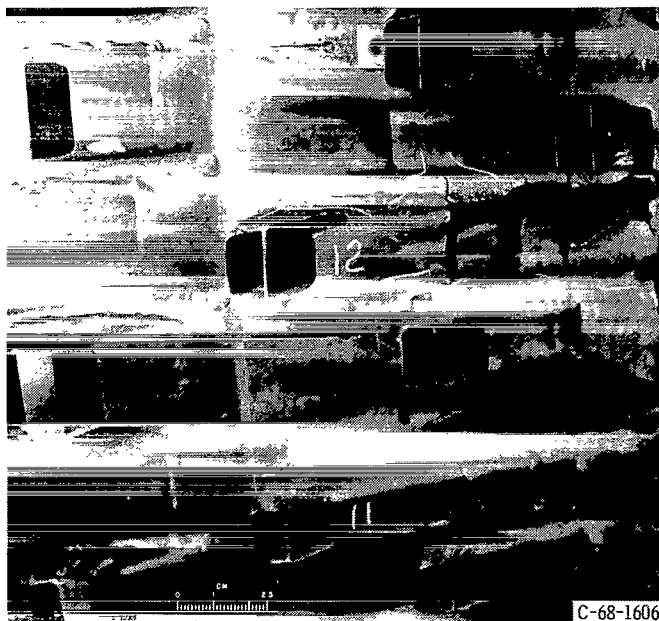


Figure 4. - Combustor and diffuser modifications - Model F.





(a) Damaged combustor inner liner.



(b) Closeup of damaged combustor inner liner and burned scoops.

Figure 5. - Damage to ram-induction combustor after 325 hours of endurance tests.

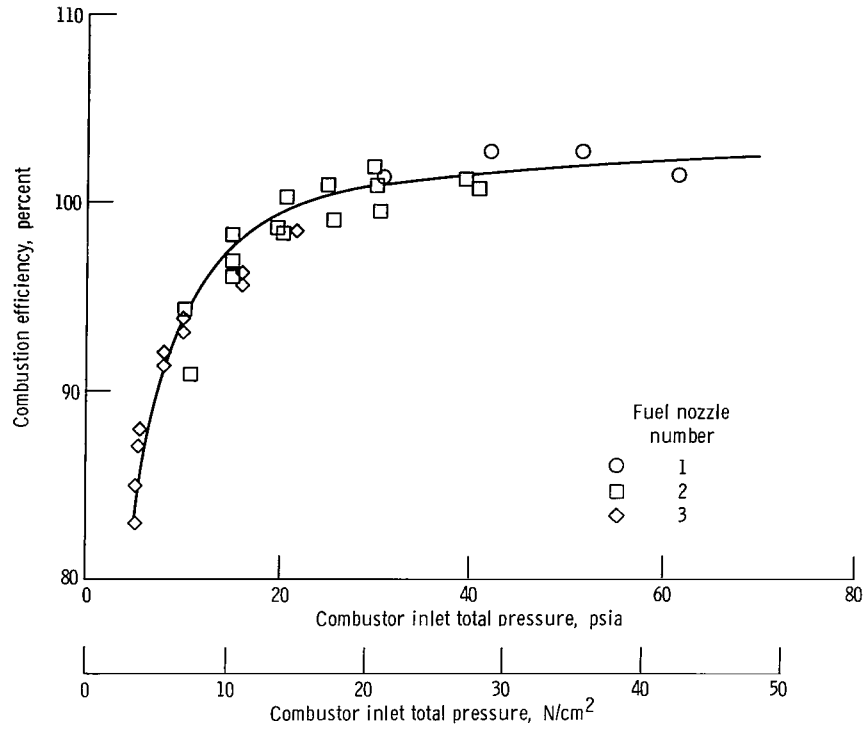


Figure 6. - Effect of inlet-air total pressure on combustion efficiency. Inlet-air temperature, 600° F (589 K); reference velocity, 150 feet per second (45.7 m/sec).

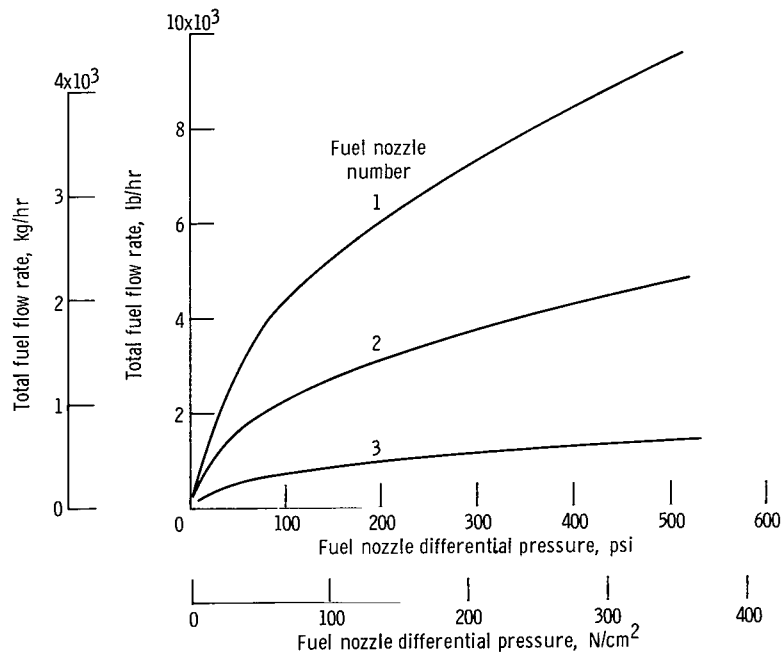


Figure 7. Flow characteristics of simplex fuel nozzles. Hollow cone, 90° spray angle.

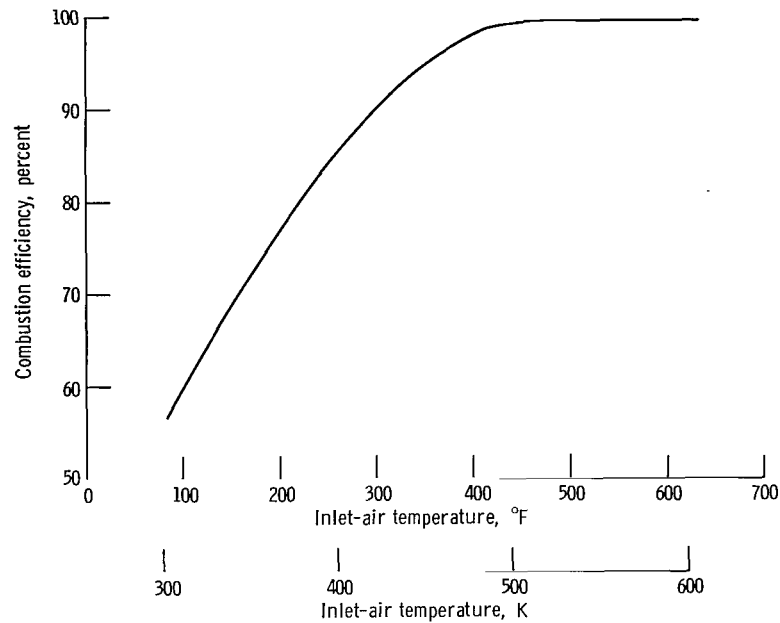


Figure 8. - Effect of inlet-air temperature on combustion efficiency. Reference velocity, 153 feet per second (46.6 m/sec); inlet-air pressure, 30 psia (20.7 N/cm<sup>2</sup>); fuel-air ratio, 0.0225; number 1 fuel nozzles.

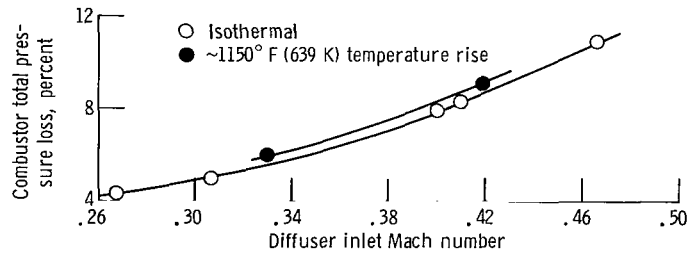


Figure 9. - Variation of combustor total pressure loss with diffuser inlet Mach number. Uniform diffuser inlet velocity profile; inlet-air pressure, 60 psia (41.4 N/cm<sup>2</sup>); inlet-air temperature, 1050° F (839 K).

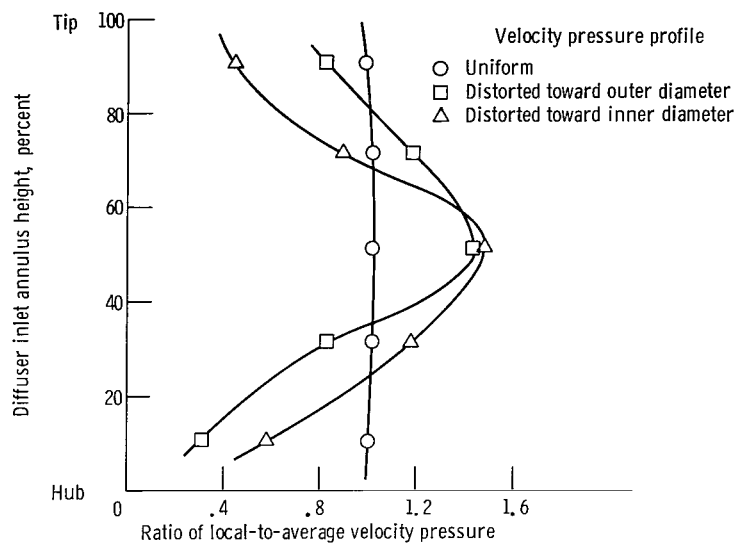


Figure 10. - Diffuser inlet velocity pressure profiles.

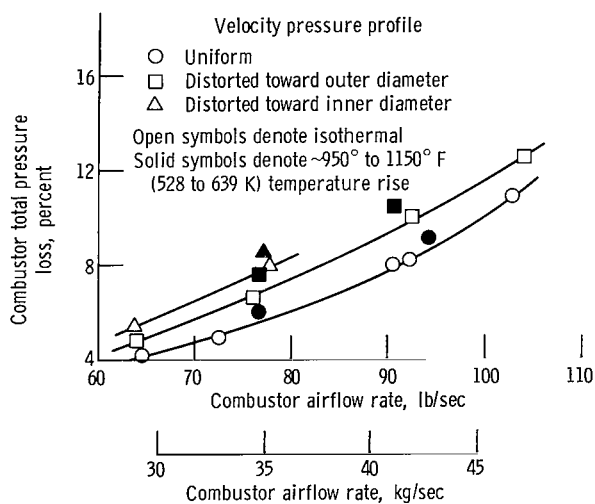


Figure 11. - Effect of inlet velocity pressure profile on combustor total pressure loss; Combustor nominal inlet conditions: 60 psia (41.4 N/cm<sup>2</sup>), 1050° F (839 K).

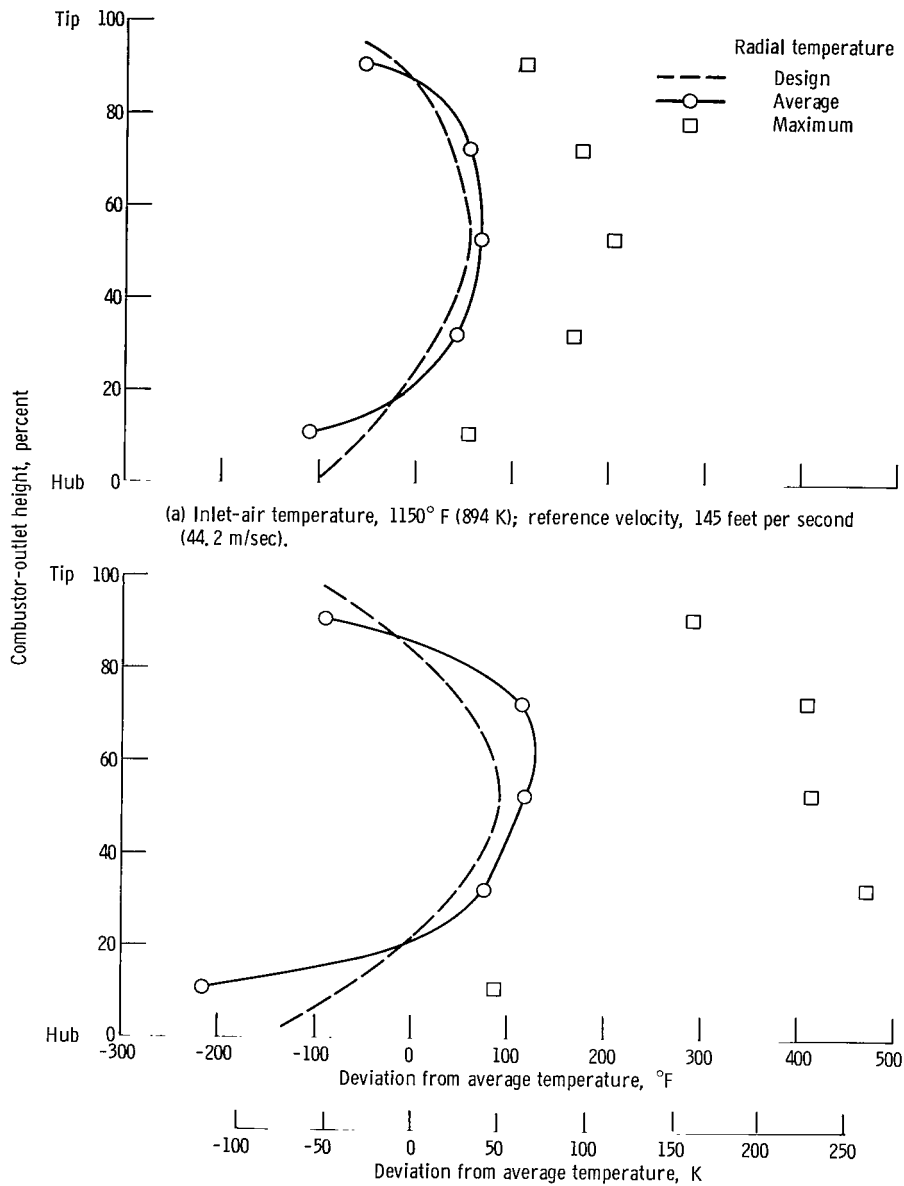


Figure 12. - Combustor average radial exit temperature profile. Inlet total pressure, 90 psia (62.1 N/cm<sup>2</sup>); exit temperature, 2200° F (1478 K). Velocity pressure profile distorted toward outer diameter.

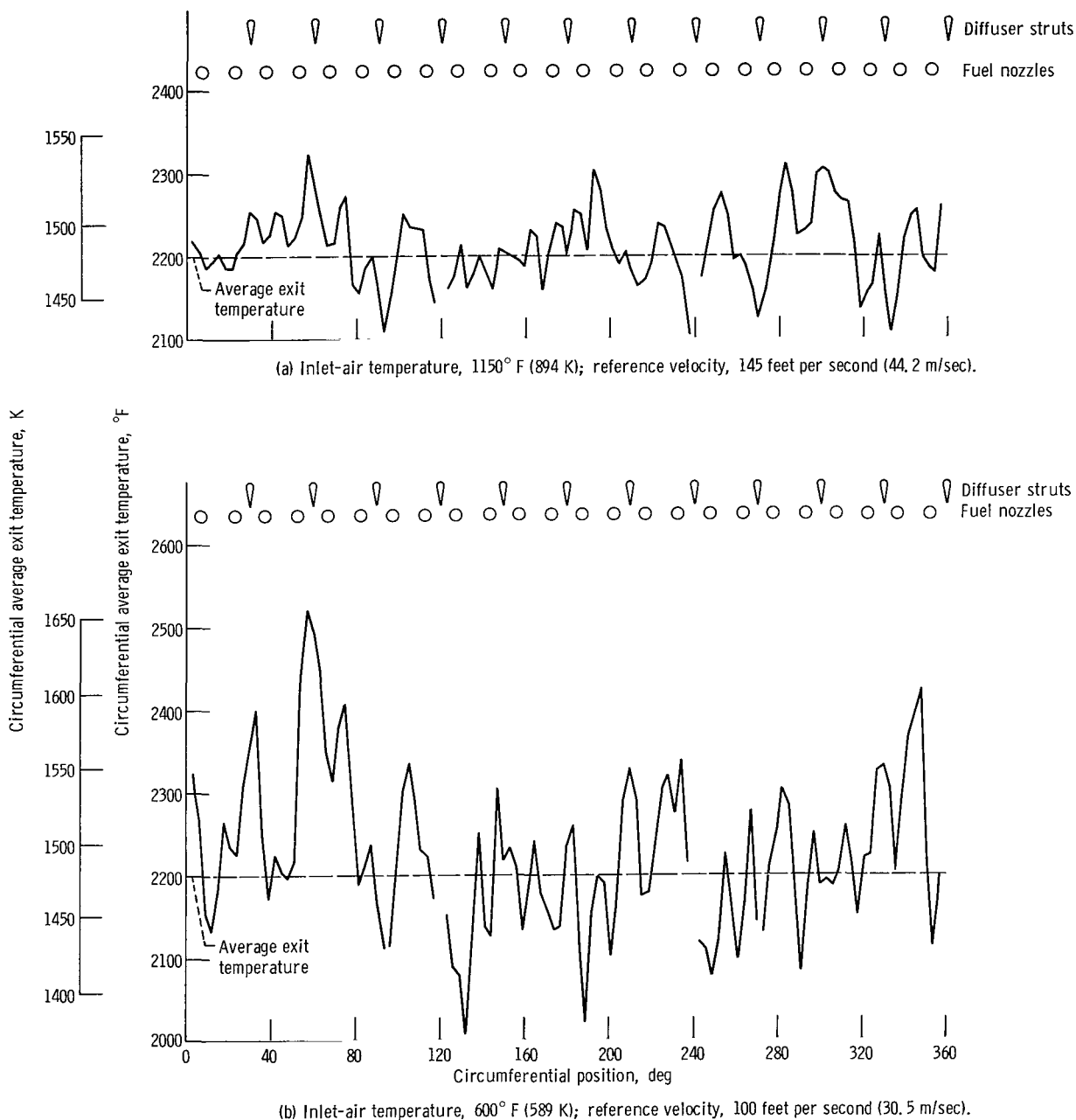


Figure 13. - Combustor average circumferential exit temperature variation. Inlet total pressure, 90 psia (62.1 N/cm<sup>2</sup>). Velocity pressure profile distorted toward outer diameter.

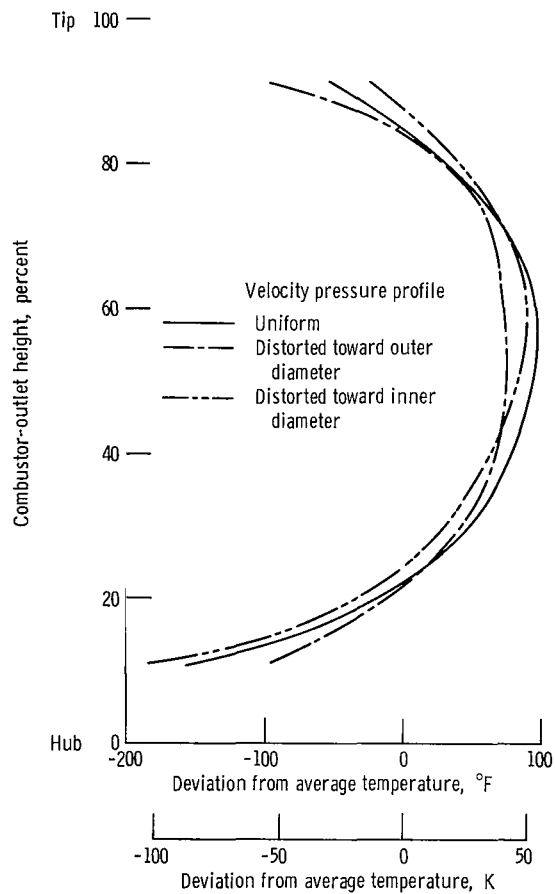


Figure 14. - Effect of diffuser inlet velocity profile on combustor average radial exit temperature profile. Inlet total pressure, 60 psia (41.4 N/cm<sup>2</sup>); inlet-air temperature, 1050° F (839 K); exit average temperature, 2200° F (1478 K); reference velocity, 125, 150, 175, and 200 feet per second (38.1, 45.7, 53.3, 61.0 m/sec).

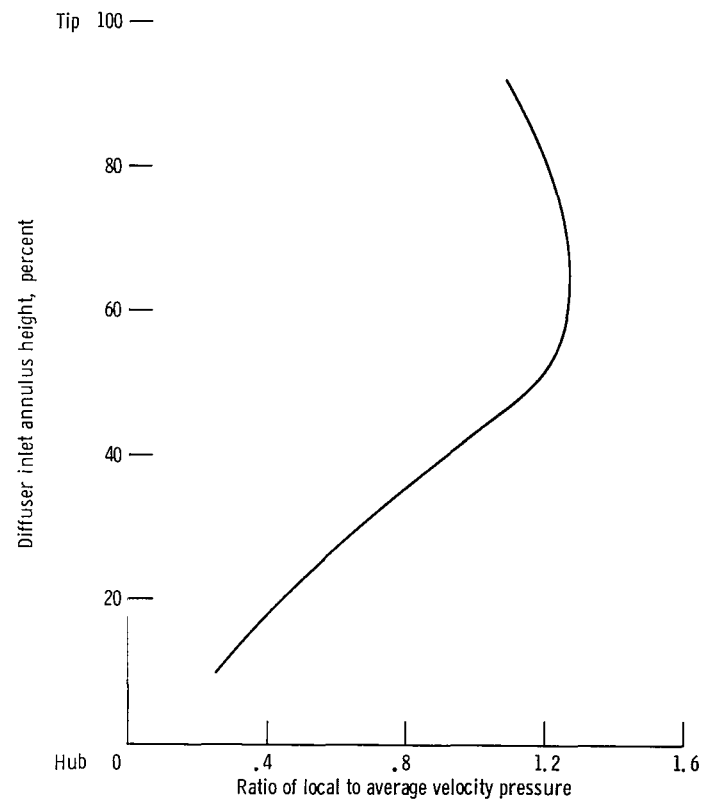


Figure 15. - Unsymmetrically distorted inlet velocity profile.

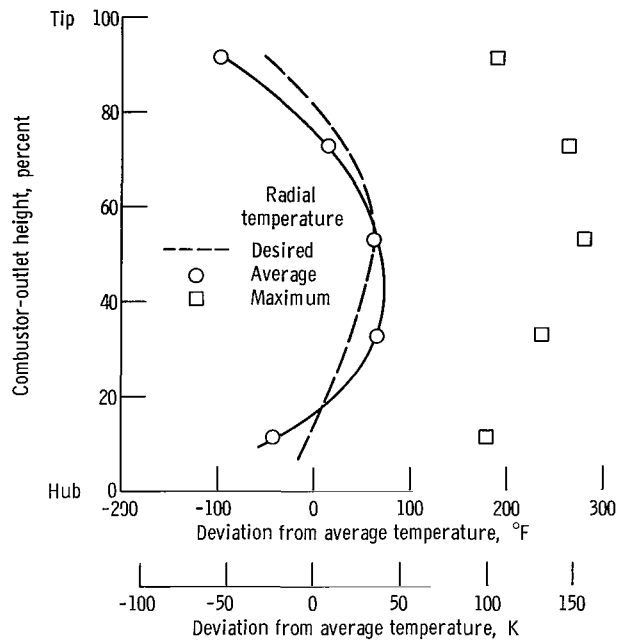


Figure 16. - Exit average temperature profile obtained with unsymmetrically distorted inlet velocity profile. Inlet total pressure, 60.0 psia (41.4 N/cm<sup>2</sup>); inlet-air temperature, 1050° F (839 K); reference velocity, 140 feet per second (42.7 m/sec); average exit temperature, 2200° F (1478 K).

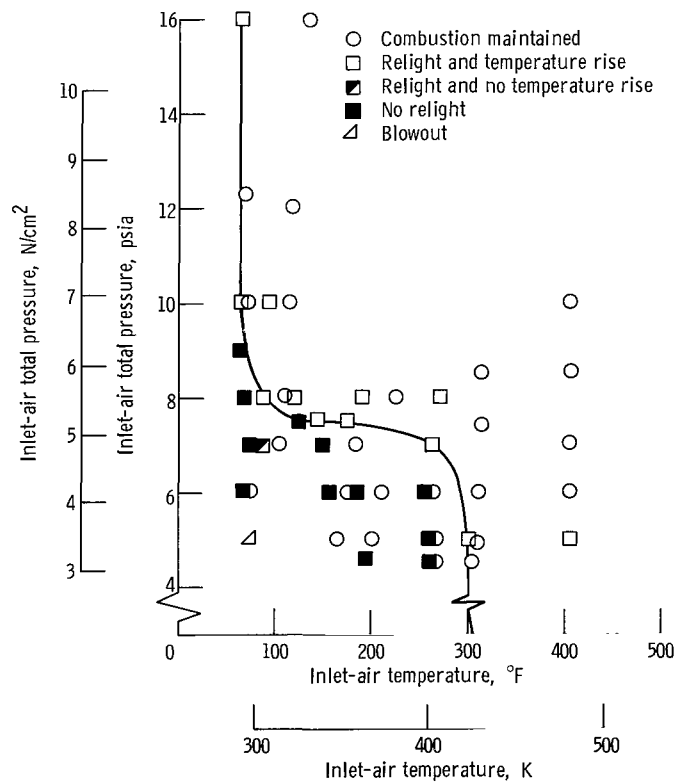


Figure 17. - Combustor blowout and relight characteristics.



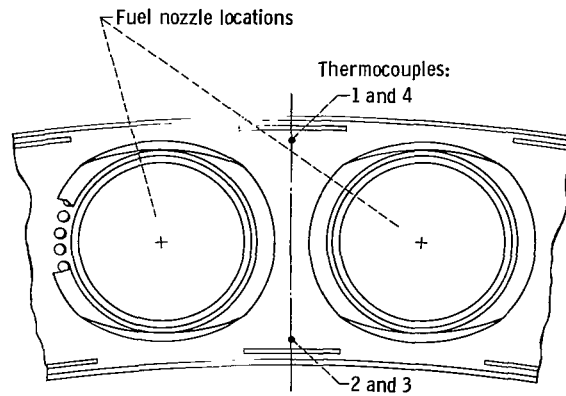


Figure 18. - Location of combustor headplate thermocouples. Looking upstream. Thermocouples 1 and 4 located on outside diameter of headplate between fuel nozzles and spaced  $180^\circ$  apart; thermocouples 2 and 3 located on inside diameter of headplate between fuel nozzles and spaced  $180^\circ$  apart.

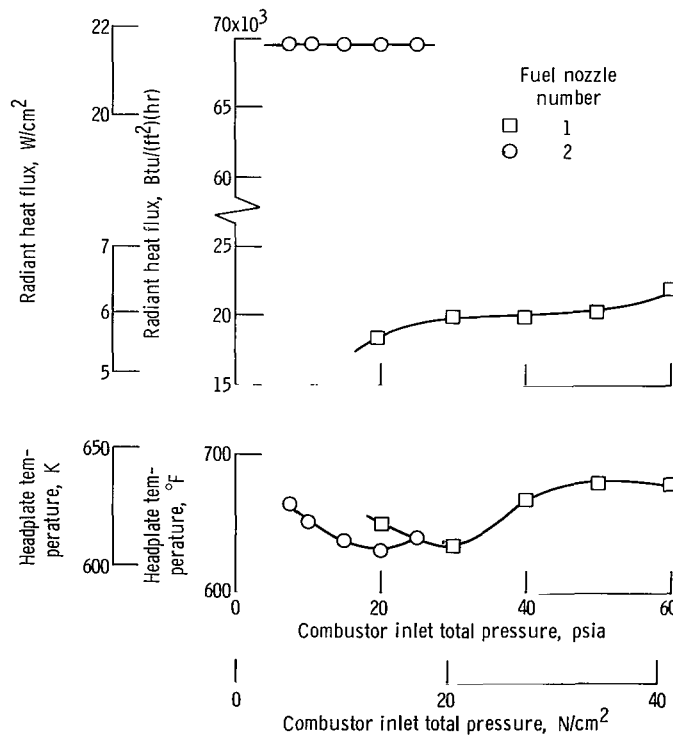


Figure 19. - Effect of combustor inlet total pressure and fuel nozzle size on headplate temperature and radiant heat flux. Reference velocity, 150 feet per second (45.7 m/sec); inlet-air temperature,  $600^\circ F$  (589 K); fuel-air ratio, 0.022.

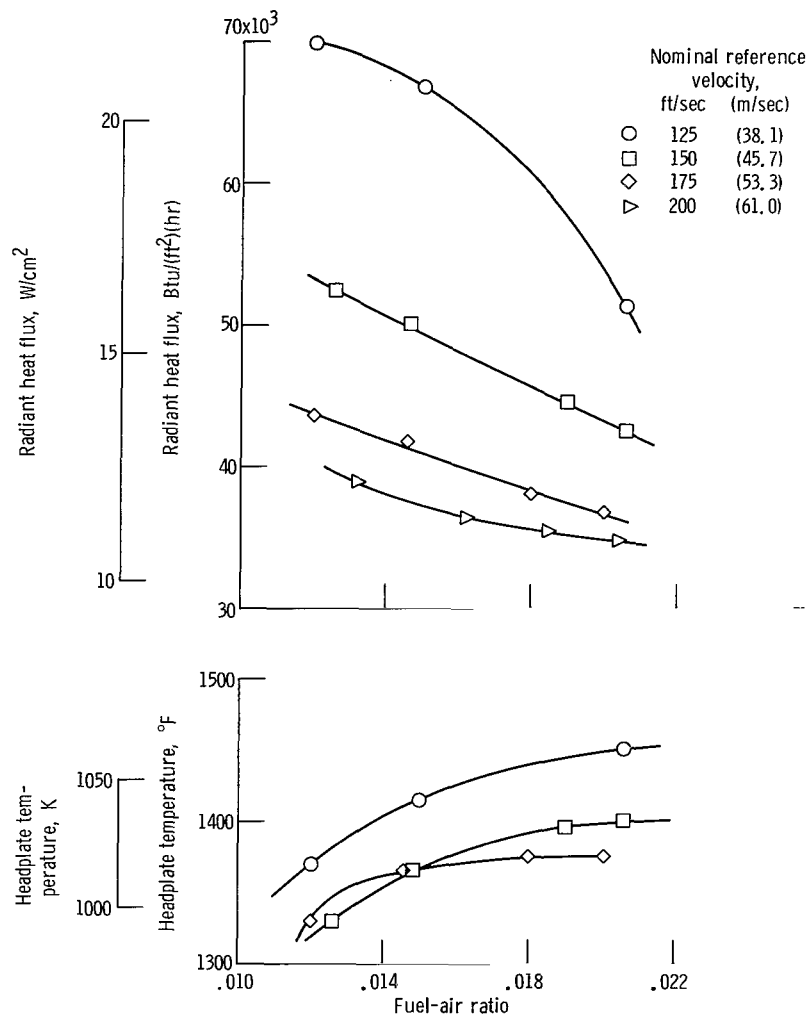


Figure 20. - Effect of reference velocity and fuel-air ratio on headplate temperature and radiant heat flux. Inlet-air pressure, 60 psia (41.4 N/cm<sup>2</sup>); inlet-air temperature, 1050° F (839 K); undistorted inlet-air velocity profile;

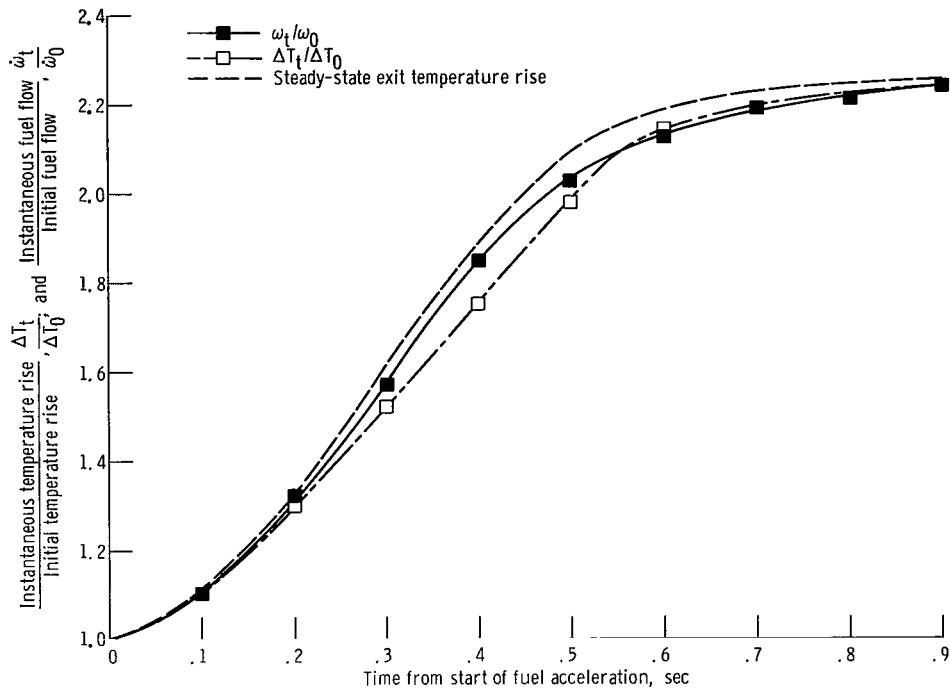


Figure 21. - Exit temperature response to rapid increase in fuel flow rate. Inlet total pressure 30 psia (20.6 N/cm<sup>2</sup>); inlet-air temperature, 600° F (589 K); initial combustor temperature rise, 590° F (328 K); initial fuel flow, 0.355 pounds per second (0.161 kg/sec).

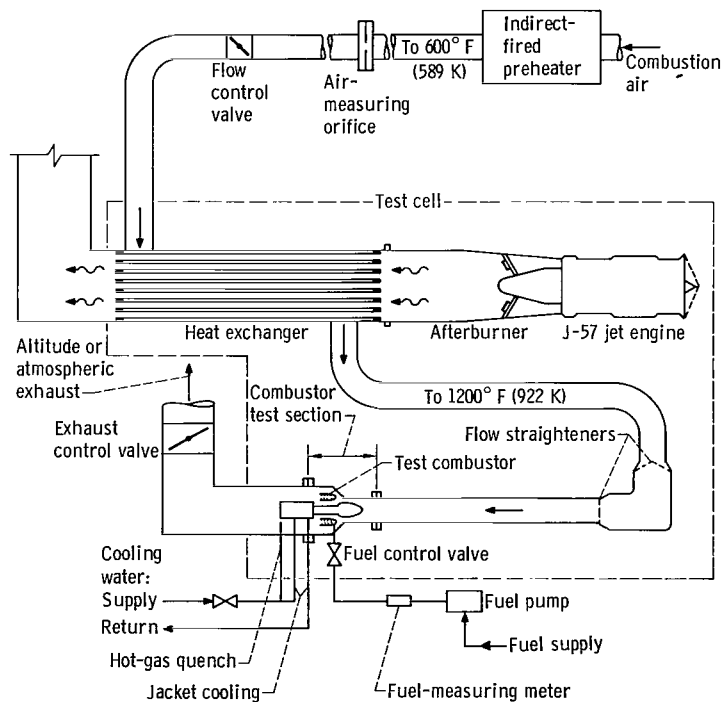


Figure 22. - Test facility and associated systems for full-scale advanced annular combustor tests.

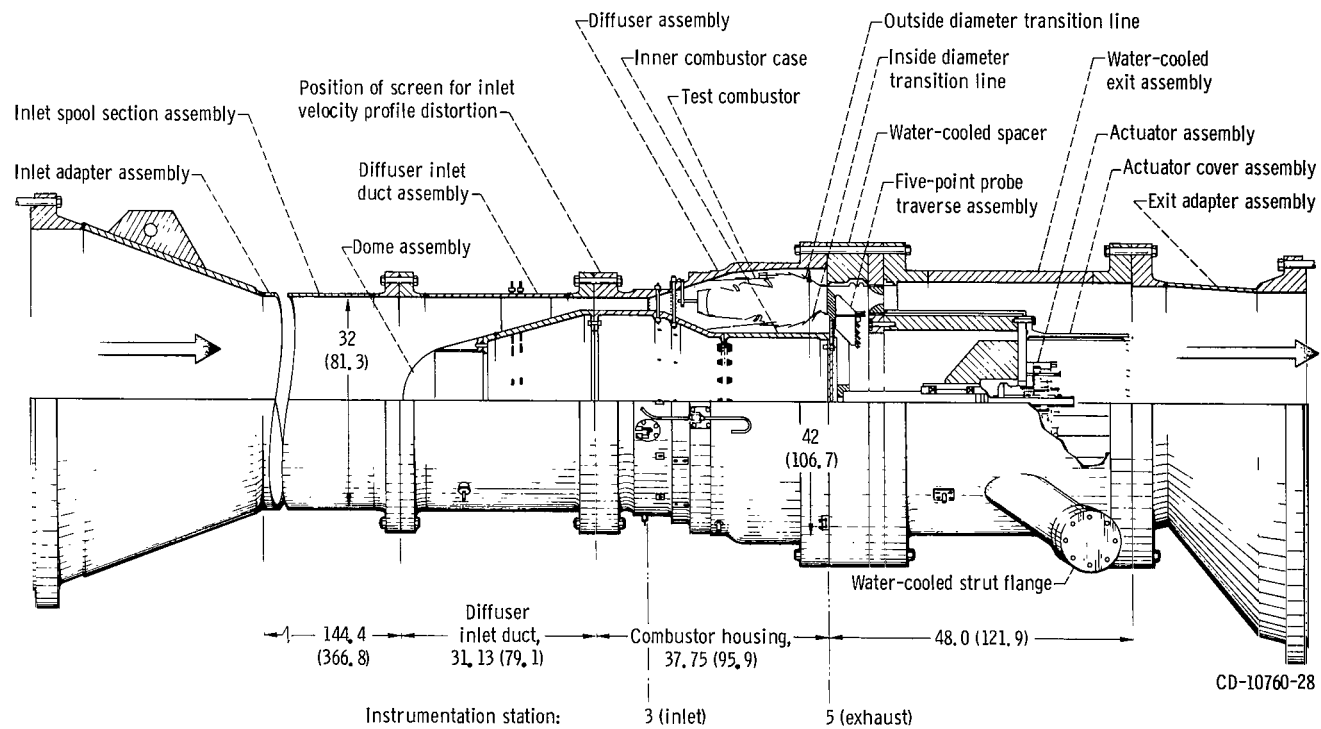


Figure 23. - Test section for full-scale advanced annular combustor. (Dimensions are in inches (cm).)

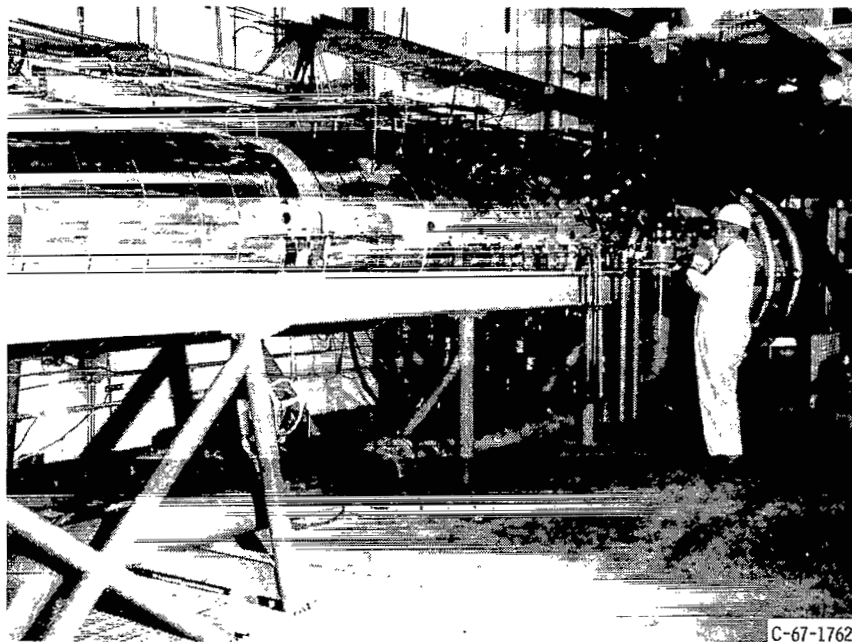
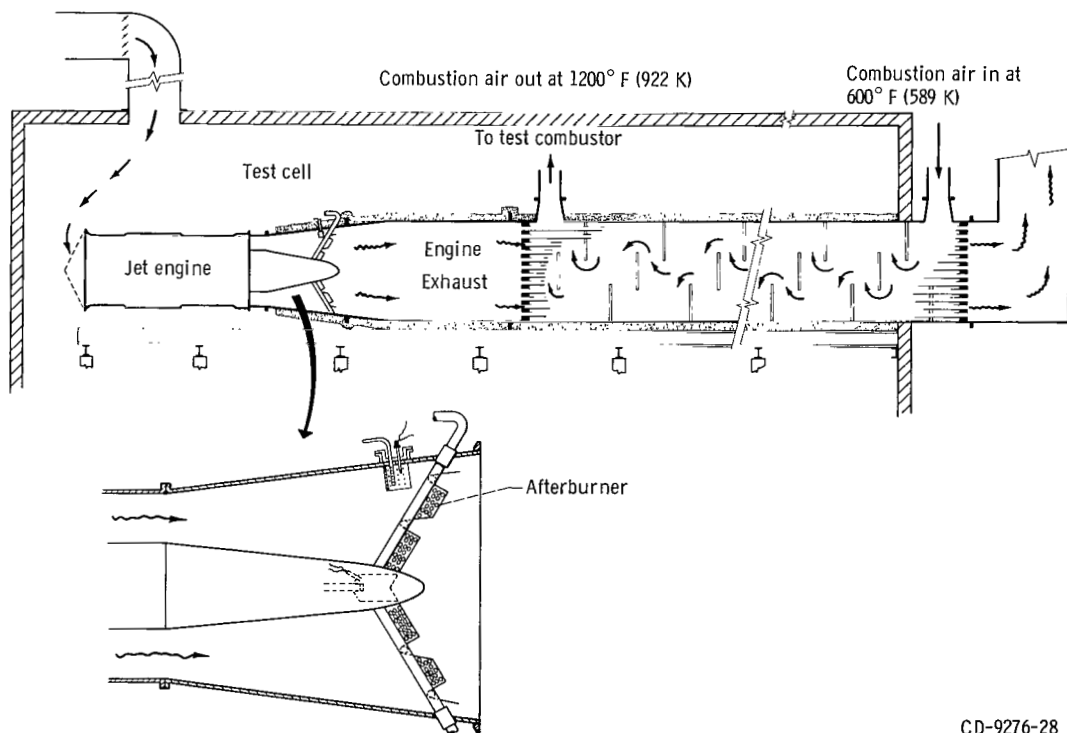


Figure 24. - Test section for advanced annular combustor.



CD-9276-28

Figure 25. - Heat exchanger in exhaust of jet engine to provide high-temperature inlet air for test combustor.

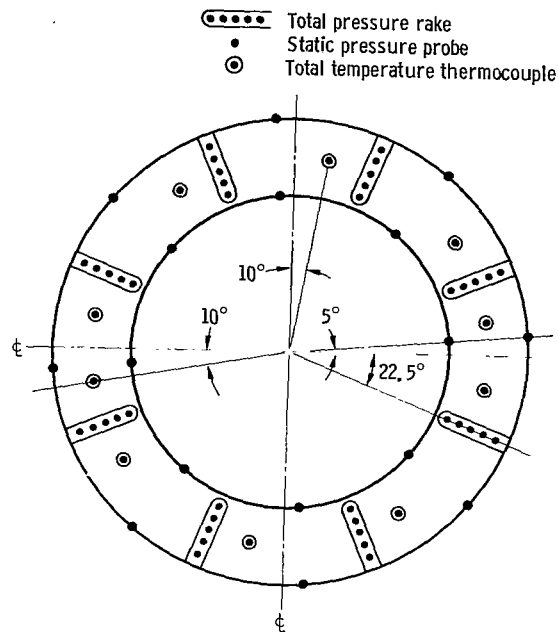


Figure 26. - Diffuser inlet instrumentation at station 3.  
View looking downstream.

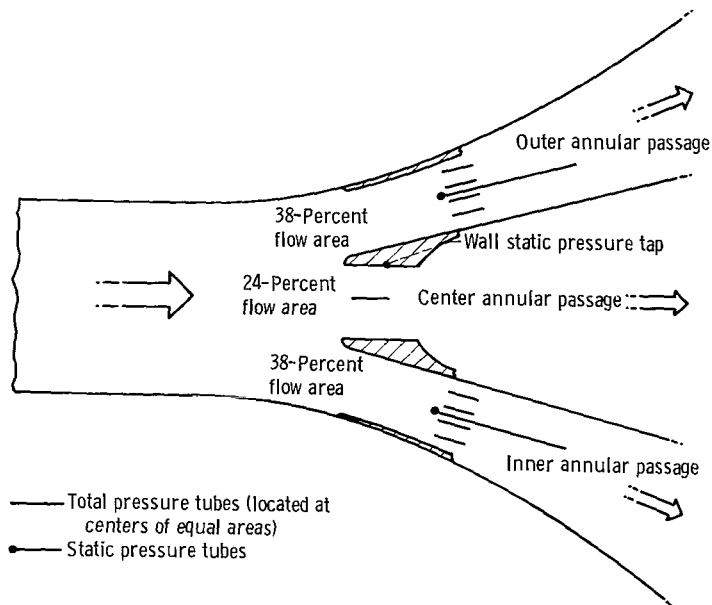


Figure 27. - Instrumentation locations for airflow measurement in combustor inlet passages.

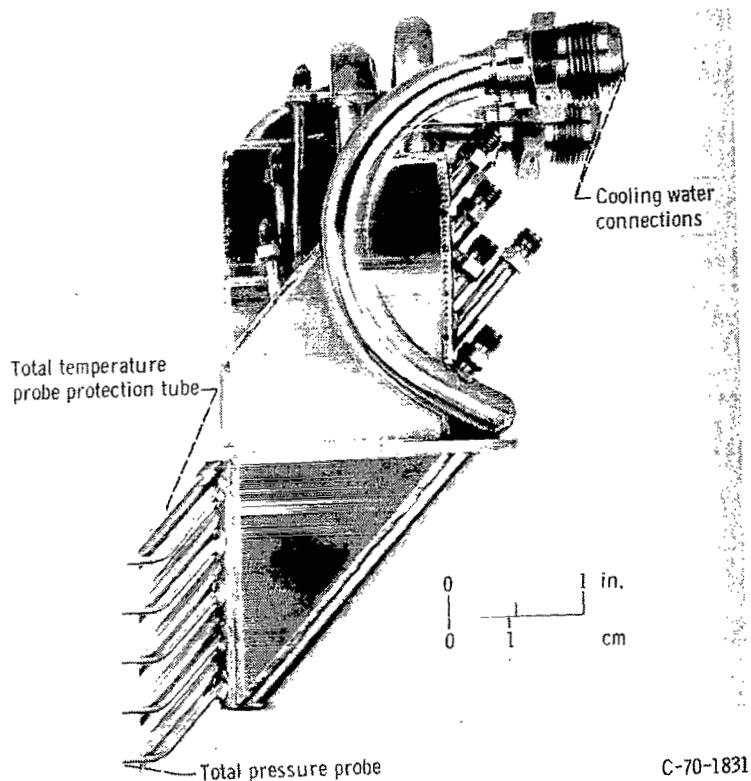


Figure 28. - Five-point total temperature and total pressure water-cooled probe assembly.

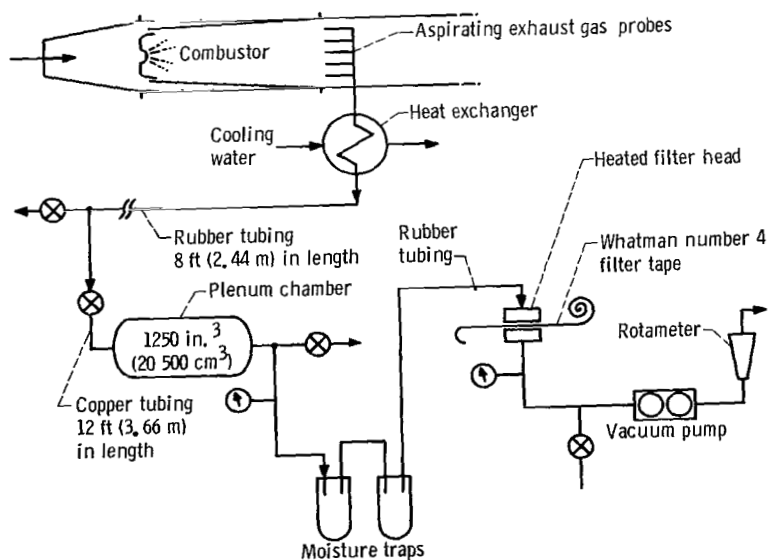


Figure 29. - Schematic of apparatus used to obtain smoke number data.

NATIONAL AERONAUTICS AND SPACE ADMINISTRATION  
WASHINGTON, D. C. 20546  
OFFICIAL BUSINESS

FIRST CLASS MAIL



POSTAGE AND FEES PAID  
NATIONAL AERONAUTICS AND  
SPACE ADMINISTRATION

04U 001 53 51 3DS 70272 00903  
AIR FORCE WEAPONS LABORATORY /WLOL/  
KIRTLAND AFB, NEW MEXICO 87117

ATT E. LOU BOWMAN, CHIEF, TECH. LIBRARY

POSTMASTER: If Undeliverable (Section 158  
Postal Manual) Do Not Return

*"The aeronautical and space activities of the United States shall be conducted so as to contribute . . . to the expansion of human knowledge of phenomena in the atmosphere and space. The Administration shall provide for the widest practicable and appropriate dissemination of information concerning its activities and the results thereof."*

— NATIONAL AERONAUTICS AND SPACE ACT OF 1958

## NASA SCIENTIFIC AND TECHNICAL PUBLICATIONS

**TECHNICAL REPORTS:** Scientific and technical information considered important, complete, and a lasting contribution to existing knowledge.

**TECHNICAL NOTES:** Information less broad in scope but nevertheless of importance as a contribution to existing knowledge.

**TECHNICAL MEMORANDUMS:** Information receiving limited distribution because of preliminary data, security classification, or other reasons.

**CONTRACTOR REPORTS:** Scientific and technical information generated under a NASA contract or grant and considered an important contribution to existing knowledge.

**TECHNICAL TRANSLATIONS:** Information published in a foreign language considered to merit NASA distribution in English.

**SPECIAL PUBLICATIONS:** Information derived from or of value to NASA activities. Publications include conference proceedings, monographs, data compilations, handbooks, sourcebooks, and special bibliographies.

**TECHNOLOGY UTILIZATION PUBLICATIONS:** Information on technology used by NASA that may be of particular interest in commercial and other non-aerospace applications. Publications include Tech Briefs, Technology Utilization Reports and Notes, and Technology Surveys.

*Details on the availability of these publications may be obtained from:*

SCIENTIFIC AND TECHNICAL INFORMATION DIVISION  
NATIONAL AERONAUTICS AND SPACE ADMINISTRATION  
Washington, D.C. 20546